Student thesis series INES nr 529

A global analysis on impact of conflicts on long-term greening trends

Mathias Welp

2020
Department of
Physical Geography and Ecosystem Science
Lund University
Sölvegatan 12
S-223 62 Lund
Sweden

Mathias Welp (2020).

A global analysis on impact of conflicts on long-term greening trends
Master degree thesis, 30 credits in *Physical Geography and Ecosystem Science*
Department of Physical Geography and Ecosystem Science, Lund University

Level: Master of Science (MSc)

Course duration: *January* 2020 until *October* 2020

A Global Analysis on Impact of Conflicts on Long-term Greening Trends

---

Mathias Welp

Master thesis, 30 credits, in *Physical Geography and Ecosystem Science*

Supervision:

Torbern Tagesson

Lund University, Department of Physical Geography and Ecosystem Science

Feng Tian

Lund University, Department of Physical Geography and Ecosystem Science

Exam Committee:

Lina Eklund, Lund University, Department of Physical Geography and Ecosystem Science

Hani Younes, Lund University, Department of Physical Geography and Ecosystem Science

Acknowledgements

Many people have in one way or another contributed to this work. First, I would like to thank my supervisors. Torbern Tagesson, for his valuable feedback, his research related inputs but especially for his optimism and encouragement throughout this project, and Feng Tian for his technical advices on GEE and programming. I want to express my immense gratitude to my mother, my brother, my other family members and my friends who supported me along the way, who always listened to my problems and who had insightful and motivating advices during my studies. Without your support the completion of this work would not have been possible. Special thanks go to my aunt Sister Magdalena Vogt, Ashish Vivekar, Shangharsha Thapa and David Kern-Fehrenbach for helping me with editing, programming or other work-related things. To my wonderful fellow students, I want to say how much I enjoyed the past two years with you and how thankful I am for your unlimited support. With your help I found a new home in Lund and I will always be happy to come back. Writing this thesis was a challenge but sharing the struggles and some cake on fika-friday with all of you made it a wonderful experience. I wish you all the best on your future endeavors.

Abstract

Armed conflicts were and are still shaping the global terrestrial land surface and can have severe direct and indirect impacts on societies, economies and the environment. This study attempts to assess the impact of armed conflicts on vegetation on global and regional scale. Four aims were formulated to scrutinize the impact of conflicts based on 1) globally distributed conflicts involving events with more than 25 deaths, 2) types of conflicts, namely: state-based violence, non-state violence and one-sided violence, 3) regional examples: Rwanda and Afghanistan and 4) levels of conflict severity by death number: greater than 0, 25 and 100. The long-term impacts were analysed by calculating linear Normalised Difference Vegetation Index (NDVI) trends in locations hit by conflicts with respect to the incident date, using an ordinary least square model. To exclude climate influence on the vegetation, over the study period of 1982-2015, the global monthly 4km climate dataset TerraClimate was used to predict NDVI in a multiple linear regression for the periods after the conflicts. It was found that conflicts have neither positive nor negative significant overall impact on vegetation on a global scale (aim 1). Between the types of conflicts (aim 2) and the death number thresholds (aim 4) no significant differences could be identified. The Rwanda results, in contrast to the Afghanistan results (aim 3) showed a disproportional amount of negative NDVI slopes, but again the slopes where not significant. In conclusion, the analysis resulted only in insignificantly small trend changes, which leads to the assumption that on this scale, conflicts have no overall strong impacts on greening.

Key words: *Physical Geography, Ecosystem Analysis, NDVI, Conflicts, UCDP, GIMMS, Google Earth Engine*

Table of Contents

List of Abbreviations

AGB ..... *Aboveground Biomass*
AVHRR ..... *Advanced Very High Resolution Radiometer*
CC ..... *Climate Controlled (Period)*
DMZ ..... *Demilitarized Zone*
ERS ..... *European Remote Sensing*
ETM ..... *Enhanced Thematic Mapper*
EVI ..... *enhanced vegetation index*
GED ..... *Georeferenced Event Dataset*
GEE ..... *Google Earth Engine*
GIMMS ..... *Global Inventory Modeling and Mapping Studies*
GPP ..... *gross primary production*
IDC ..... *Internally Displaced Person*
IQR ..... *Interquartile Range*
LAI ..... *Leaf Area Index*
MVC ..... *Maximum-Value Composite*
NDVI ..... *Normalized Difference Vegetation Index*
NIR ..... *Near Infrared Radiation*
NOAA ..... *National Oceanic and Atmospheric Administrations*
P ..... *Precipitation*
PAR ..... *Photosynthetically Active Radiation*
SAR ..... *Synthetic Aperture Radar*
SM ..... *Soil Moisture*
SRTM ..... *Shuttle Radar Topography Mission*
Std. Dev ..... *Standard Deviation*
T ..... *Temperature*
tmmx ..... *Maximum Temperature*
TRMM ..... *Tropical Rainfall Measuring Mission*
UCDP ..... *Uppsala Conflict Data Program*
VI ..... *Vegetation Index*

List of Figures

List of Tables

1 Introduction

In post-World War II and Cold War time decentralized armed conflicts in different forms are taking place around the globe with 40 active wars on four continents in 2014 (Baumann and Kuemmerle 2016) and a total number of 259 wars since the World War II (Pettersson and Wallensteen 2015). 80% of the major armed conflicts between 1950 and 2000 took place in biodiversity hotspot areas (Hanson et al. 2009) and 55 of the 70 conflicts in 2009 in developing agrarian economies (UN-HABITAT 2012). The extent of conflicts is usually described in terms of effects on human systems like casualty numbers, economic loss, areas of destroyed buildings or cities, or by estimates of displaced people. Limited attention is given to the long-lasting effects of war-related environmental effects of armed conflicts (Baumann and Kuemmerle 2016). This topic should not only be of great interest due to the loss of biodiversity and the disruption of protected areas but due to the resulting increased pressure on human systems by the reduction of essential ecosystem services, especially the access to safe water, which is additionally altered by climate change in many regions (Oppenheimer et al. 2015). Food security, water, fuel and wood availability, protection against natural hazards, forage production, crop pollination to mention only a few of the services provided by ecosystems to support societies (Fisher and Turner 2008; Chan et al. 2006). With three of seven global environmental system boundaries already exceeding their thresholds (Rockström et al. 2009), limiting further pressure on these systems is key for the functioning of the global environment (Francis and Krishnamyrthy 2014).

The relationship between the environment and conflicts is complex and reciprocal. Environmental degradation and resource scarcity can increase the likelihood of conflicts and the human history is full of examples of war to gain land, energy supplies or other environmental resources (Brundtland 1987). On the other hand, there are countless examples of direct and indirect effects of armed conflicts on vegetation and wildlife (Dudley et al. 2002; Hanson et al. 2009; Brown 2010; Baumann and Kuemmerle 2016; Francis and Krishnamyrthy 2014; Stevens et al. 2011). This mutual relationship is underrepresented in research, especially concerning systematic ways of using quantitative methods (Gleditsch 1998).

In the field of remote sensing there were many attempts to assess environmental changes as a result of armed conflict. Early in the 1980s remote sensing (Landsat MSS imagery) was used to identify land-use change as a product of war-related land abandonment (Witmer 2015). However,

to quantitate the effects of conflicts on the environment, especially using spectral satellite data, more scientific attention is needed and with increasing computation capacity and data availability more extensive analysis is possible. Since investigating conflicts on the ground is often difficult due to restricted access (Witmer 2015), remote sensing is a widely used tool for researchers and the military (Gorsevski et al. 2012). Especially since the Gulf War (1990 – 1991, Iraq - U.S.-led coalition), the so-called 'first space war', new techniques for monitoring conflicts remotely were tested (Anson and Cummings 1991).

One indicator of vegetation health is derived by measuring its ability to absorb and use Photosynthetically Active Radiation (PAR). Canopy reflectance can be measured by satellite sensors by detecting the reflected surface radiation. A common approach for identifying vegetation status is to calculate vegetation indices by combining information in different spectral bands (Xue & Su, 2017). The normalized difference vegetation index (NDVI) is the absolutely most common satellite based vegetation index, and is a proxy of vegetation greenness (Xue and Su 2017). It is selected because it only needs two bands, which were already measured in 1981 with the launching of the Advanced Very High Resolution Radiometer (AVHRR) instrument. Due to this long time span of vegetation data reaching back to the early 1980s (Tucker et al. 2005), the trend analysis in this study is specified as 'long-term', following other similar studies (Tian et al. 2015; Gutman 1999; Liu et al. 2019). It is based on greening trends for periods of up to 17 years. Using satellite data from early sensors (especially AVHRR), these study periods are usually specify as 'long-term'. The ratio between the visible and the near infrared radiation (NIR), radiances shows the photosynthetic capacity. The higher the ratio, the more photosynthetically active the vegetation cover (Sellers 1985).

For areas affected by human conflict, a global scale vegetation analysis will be conducted based on a NDVI image collection provided by the National Oceanic and Atmospheric Administration (NOAA) corrected to decrease non-vegetation effects (Pinzon and Tucker 2014). The image collection 'NASA/GIMMS/3GV0' will be analyzed in the web-based remote sensing platform, Google Earth Engine (GEE). To control the resulting trend for climatic changes the data will be normalized against variability in temperature, precipitation and soil moisture.

This study does not attempt to find causal relationships between conflicts and environmental degradation or increase in greening, but rather attempts to find measurable greening trends in conflict regions over the last three decades. This is mainly because armed conflicts, especially civil

conflicts, which represent the main type of conflict over the study period, are exacerbated by multiple complex causes (Brown 2010). The main objective of this study is to quantify changes in vegetation greenness in areas of human conflicts. The research questions addressed in this project are:

1) Do conflicts globally have a measurable impact on vegetation greenness (NDVI)?
2) Do distinctive types of conflicts affect the vegetation greenness differently?
3) Can differences in NDVI trends be identified between the genocide in Rwanda (1994) and the Afghanistan War (2001-2008)?
4) Do fatality numbers of incidents affect the greening?

The hypothesis of a negative correlation between conflicts and greening on a global scale will be tested.

2 Background

2.1 Conflict terminology

Several terms are used to define the settlement of disputes or the 'contested incompatibility' using arms (not restricted to modern manufactured weapons, but also including sticks, stones, fire etc.), depending on the parties involved and the number of casualties in a certain period (usually one year). The conflict terminology for this project is oriented on definitions and terms from the Uppsala Conflict Data Program (UCDP) by Uppsala Universities' Department of Peace and Conflict Research (Sundberg and Melander 2013b). It is, "the world's main provider of data on organized violence" (UCDP 2020b) including an almost 40-year-long ongoing civil war data collection.

In the UCDP GED (19.1) database, these 'events' are spatially and temporally specified (Högbladh 2020), with each event georeferenced (WGS 84) and dated. In this dataset a lethal 'event' is defined as an "incident where armed force is used by an organized actor against another organized actor, or against civilians, resulting in at least one direct death at a specific location and a specific date" (Högbladh 2020, p. 4), herein referred to as event or conflict.

Different types of conflicts are specified by UCDP, namely: wars, armed non-state, interstate, intrastate and intrastate conflicts with foreign involvement, which will be titled 'conflicts' in this study. Note that the only exception are paragraphs concerning question 2 (Chs.: 4.2.3, 5.2, 6.2),

which focuses on the three different types. More information on these terms and definitions can be found in UCDPs Codebook (Högbladh 2020).

Referring to UCDPs terminology, the term 'armed conflict' defines the 'contested incompatibility', where armed forces of at least two parties, are active and result in at least 25 'battle-related deaths' within one calendar year. A 'war' is defined as conflict resulting in at least 1000 battle-related deaths in a calendar year, involving at least one state government.

2.2 Global conflict trends

There are several long-term global conflict trends. A rising number of civil conflicts during the Cold War between 1960 and 1990 and a rise of civil conflicts with foreign state intervention in the last decade, resulting in 52 conflicts counted in 2015, the highest total number of conflicts (Fig 1) and a decreasing trend of averaged deaths per conflict (Fig 2). The face of conflicts, therefore, has changed in the last decades, from being extensive wars between or involving 'great powers', to smaller, decentralized conflicts often involving non-governmental groups. Although these armed conflicts are smaller in size, they are severe shocks and can have far reaching effects on societies as well as the environment (Baumann and Kuemmerle 2016).

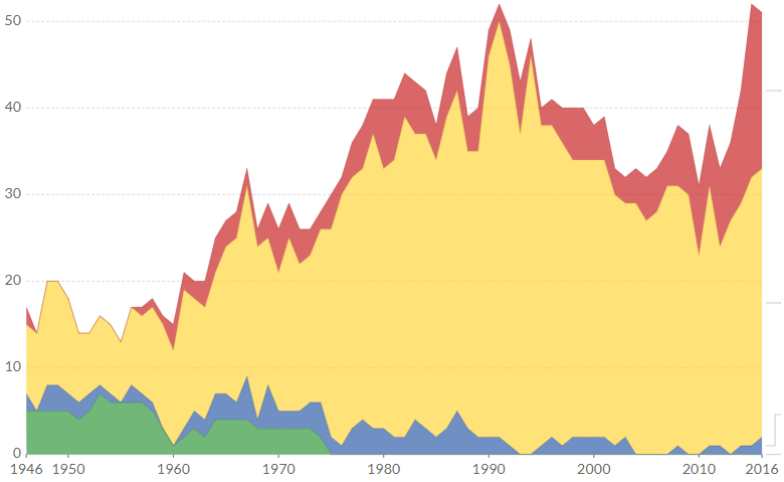

Figure 1 Number of conflicts between 1946-2016 by type: green) colonial or imperial conflicts, blue) conflicts between states, yellow) civil conflicts, red) civil conflict with foreign state intervention. All involving at least one state government. Re-produced from Roser (2016) with permission from publisher UCDP.

Other trends like population growth and urbanization are altering land cover. Smith et al. (1999) state that environmental degradation contributes to conflicts. However, the complex interdependence of conflicts and the environment is discussed widely and there is no overall agreement whether environmental degradation causes or contributes to conflicts (Brown 2010). The opposition criticizes that supporting studies are based on static perceptions of the environment and that eco-scarcity as a cause of conflict is difficult to prove or disprove. The high complexity of many conflicts, including factors such as population growth, urbanization, disease, technological overextension, ethnicity and religion, climate change, environmental degradation, resource scarcity (i.e. food, water and fuel shortage) make it difficult to conclude on a single main factor as cause of a conflict (Urdal 2005; Raleigh and Urdal 2007; Brown 2010; Flint 2009; Byers and Dragojlovic 2004).

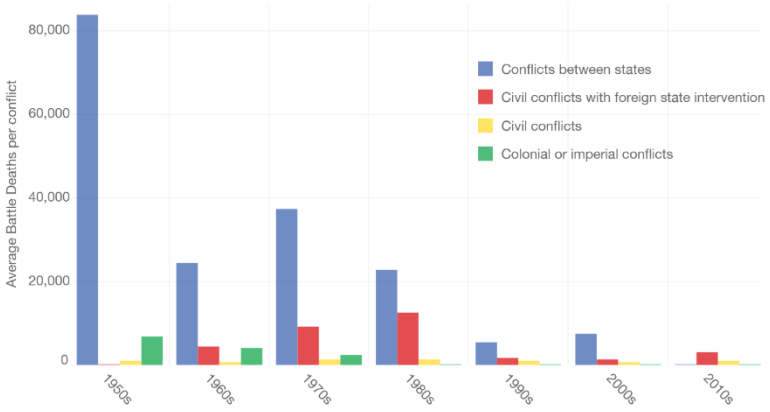

Figure 3 Average number of casualties by conflict (with more than 25 annual deaths) between 1946 and 2016 by type. Re-produced from Roser (2016) with permission from publisher UCDP.

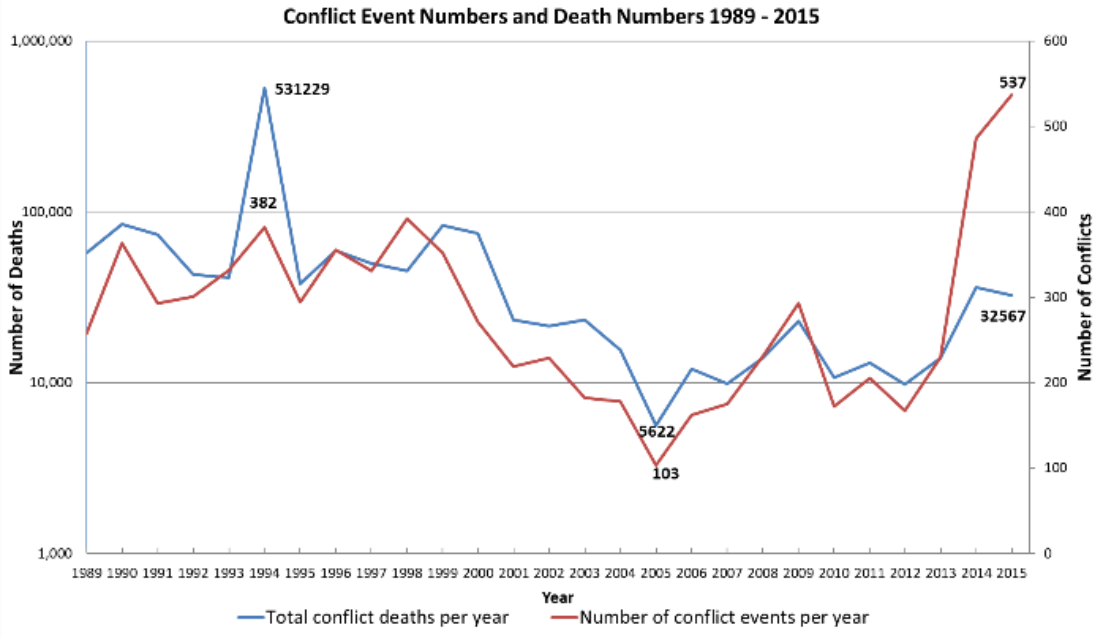

Figure 2 Comparison of conflict death numbers by year in the study period (blue line) and the according number of conflicts (red line). Note that the left y-axis (for the blue line) is a logarithmic scale. Based on data from UCDP (2020a).

More conflicts do not necessarily mean more deaths. As discussed above, the last three decades saw high numbers of conflicts but a decrease in the number of deaths per conflict. In the study period (1989 – 2015) the (Pearson) correlation between these two variables is strong (r = 0.33), as with higher numbers of conflicts there are generally more conflict deaths. However, the prominent types of conflict, the locations and other variables change as well, which alters this correlation. Two examples of a low correlation are the genocide in Rwanda and the 2015 peak in conflict numbers (Fig 3). In relatively few events (249) the highest death number is counted in 1994**,** with 501961 of the total 531229 deaths in Rwanda. The other extreme is the peak number of conflicts in 2015 with 537 events compared to relatively moderate numbers of deaths (32567) in the same year.

In addition, it is important to keep the spatial distribution and the extent of the conflict events in mind. Looking at the time frame of this study, one observes how the share of conflicts per continent changes significantly with the threshold of the number of deaths included (Fig 4). If all conflicts were included (deaths >0) Asia's share (excluding the Middle East) of all worldwide conflicts is 47% and Africa's is only 26%, but with increasing the threshold to 25 and 100 deaths, Africa's total share increases to 48% and 62% and Asia's decreases to 29% and 22% respectively. In conclusion, it is evident that the highest number of conflict events are in Asia, but the highest number of extensive deadly events is found to be in Africa.

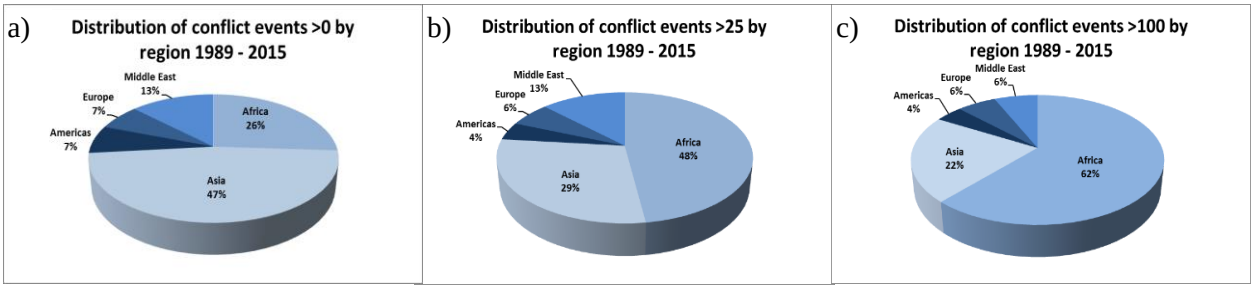

Figure 4 Distribution of conflict events by region with a) >0, b) >25 and c) >100 deaths. Based on data from UCDP (2020a).

.

2.3 Negative effects of conflicts on the environment

Armed conflicts are strongly interlinked with the environment, by either contributing to tensions due to limited resources or by destruction of ecosystems as side effect or as conflict strategy to affect local livelihoods (Stevens et al. 2011). Witmer (2015) identifies a varying time delay of conflict effects, making it difficult to link them to conflict events. Remote sensing technology is used both to assess destruction of urban areas and environmental degradation as results of conflicts.

For short-term and long-term effects on the society or the environment, a wide range of sensors and methods are used to assess these damages (Witmer 2015). The key difference however is the 'time delay of the visible manifestation' of these damages. Damage on urban structures are usually assessed in the immediate aftermath, whereas environmental damages, like forest fires or oil well fires (Gulf War) are long term effects, often lasting for hours or days after the incident (Witmer 2015). War induced land-use changes can go on for months or even years. One example is the widely seen phenomena of war related reforestation and deforestation. A study by Stevens et al. (2011) detected reforestation of areas affected by the civil war in Nicaragua from 1978 to 1993 due to displacement, followed by intensive deforestation, in the years after the civil war.

Examples of direct effects of conflicts are the defoliation in the Vietnam war, which changed large areas of tropical forest into grasslands (Dinh 1984), the intense bombardments of defensive lines at the western front in World War 1, which created a long battle stripe absent of vegetation in France or the intentional triggering of fires in Darfur, Sudan (Witmer 2015; Bromley 2010). Indirect effects of war are linked to the fact that environmental protection is often of low priority in war times (Hanson et al. 2009). Biodiversity loss is therefore often a result of decreased guarding of protected areas (Hanson et al. 2009). Refugees fleeing from conflicts to other countries or other forms of displacement like IDCs (internally displaced person) can increase environmental pressure on the hosting region, by additional exploitation of the surrounding environment to build houses or for cooking (Maystadt et al. 2020). In a study by Maystadt et al. (2020) a correlation between displacement (refugee camps) and land-use change (forest to cropland) was found, indicating an increase of 1.4 % in agricultural land with an increase in the number of refugees by 1%. However, it is noted that this strongly depends on local conditions, like the provision of vital goods by the hosting country and therefore differs strongly.

2.4 Positive effects of conflicts on the environment

Conflicts can lead to positive 'release' effects on the environment by reduced pressure and decreased exploitation of natural resources (Hanson et al. 2009). A prominent example is the Demilitarized Zone (DMZ) between North and South Korea. In this inaccessible 4 km wide and 250 km long corridor (located in a 5-20 km wide buffer zone), Koreas biodiversity was partly preserved, forest was rehabilitated and farmlands returned to a natural state (Kim 1997). Other observations of nature preserved or recovered due to conflicts can be found in Europe after the

world wars (Smith 1996), in Myanmar (Rabinowitz 2005), in Nicaragua (Nietschmann 1990), in New Guinea and in the Amazon (McNeely 2003). In most cases nature was preserved basically due to the long-term absence of human activity in these areas. The dispersion of land mines as a remnant of conflicts or insurgent activities can lead to land abandonment by the local community and can give the local flora and fauna the chance to reconquer the land (Hanson et al. 2009; Martin and Szuter 1999). However, this effect can only be seen in a few conflicts in the last decades. In most cases the short-term benefits for wildlife, e.g. due to migration or displacement which can limit human influence inside the war zone, is outweighed by the economic and social aftershocks of conflicts, leading to negative long-term effects. Additionally, during conflicts, increased poaching (by refugees, military or civil groups), and exploitation of natural resources for shelter, food or fuel can have large impacts on wildlife and the environment (Dudley et al. 2002).

2.5 Land use change and effects

Large parts of earths terrestrial surface are managed by humans. This includes urban areas, agricultural land, pastures, forests and even national parks, where fuel management or dead wood removal is often practiced for wildfire prevention (Fernandes and Botelho 2003). Land-use change can therefore affect large areas, with potential feedbacks on the local environment. This can even alter local climates. A prominent example for this is the Brazilian Amazon, which saw increasing deforestation under the current president Jair Bolsonaro (Escobar 2019). Model results show that the massive deforestation in the amazon leads to reductions in precipitation, evapotranspiration, and cloudiness and has also remote effects on other parts of the globe (Werth and Avissar 2002). Shifts of political systems for example from authoritarianism to democracy or from a centralized to a decentralized political authority, or socioeconomic shifts for example towards deregulation can have strong consequences on the environment (Prescott et al. 2017). These political changes are often results of conflicts like civil wars and can lead to widespread deforestation, apparent in Myanmar and Indonesia but also other parts of the world (Prescott et al. 2017). Land-use change due to wars by influencing land-use decisions are discussed by Baumann and Kuemmerle (2016). An example for major conflict related land-use change is the widespread abandonment of agricultural land after the collapse of the Soviet Union (Schierhorn et al. 2013), where in some regions in 2006, in comparison to the 1990s, only 49% of the land was still used

(de Beurs et al. 2017). The interlinkages between local land-use change and their effects on the environment, and the fact that there is still a great number of ongoing conflicts worldwide influencing land-use decisions, should motivate for research in this area. Baumann and Kuemmerle (2016) conclude that the importance of understanding how wars alter land-use decisions is not reflected in research. According to the IPCC several changes of the climate system which drive land degradation are already observed and will continue to intensify. Among them are changes in precipitation patterns including higher intensity and frequency of heavy precipitation (medium confidence), increased heat stress (high confidence), increased drought frequency and severity (medium confident) (IPCC 2019). These changes combined with human activities can lead to increased desertification and land degradation (note that estimates of the extent of global land degradation involves uncertainties and multi-method approaches which are rated with very low confidence) (IPCC 2019). Land degradation reduces agricultural productivity, and therefore, in combination with population growth, increases the pressure on societies and can lead subsequently to a higher number of conflicts, assuming that conflicts over resources, as described by Brundtland (1987) are continuing to occur. However, it must be noted that trends of these natural and socioeconomic systems vary strongly by region. The lack in understanding how conflicts influence the environment can therefore be understood as an additional uncertainty, limiting our ability to predict future land-use change (Müller et al. 2014). In a study by Müller et al. (2014), shifts of natural stable regimes, from one equilibrium to a new one, were investigated for countries in Southeast Asia. In their quasi-equilibrium phase system characteristics like carbon dynamics or biodiversity remain stable. Anthropological drivers like population growth or political changes can lead to gradually increasing pressure on land systems, until a threshold is exceeded, and a new state is reached. However, it must be noted that the vegetation, which will be the research object of this study, is only one of many influencing elements of the climate system (Le Treut and Somerville 2007), and it exceeds this studies scope to scrutinize the climate effects of conflict induced land-use change.

2.6 Global environmental and climate trends over the period

Besides anthropogenic trends like land-use change, population growth, urbanization and conflicts, the natural systems have changed as well during the study period, amplified by human activities. To verify the identified vegetation trends in the conflict regions interpolated climate data on

surface temperature, precipitation and soil moisture will be used in a regression analysis. However, a brief look at other climate data during the study period is necessary to address the results of this study later on.

Figure 5a shows the global temperature trends during the last three decades. Warming, indicated by red areas, is dominating the surface temperature. However, warming is not equally distributed, due to natural factors like the polar amplification. Regional conditions can even lead

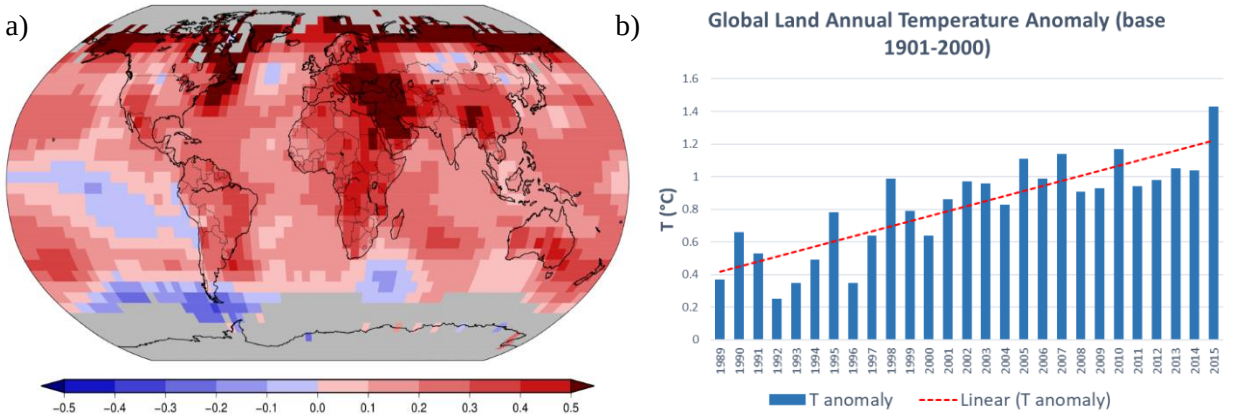

Figure 5 a) Annual global surface temperature trends averaged per decade and grid cell between 1990 – 2019. Red grid cells imply temperature increase, blue temperature decrease, and grey missing data, compared to the 1901-2000 base period. Based on data from NOAA (2020c) with permission from publisher NOAA. b) Global temperature (T) anomaly on land between 1989 and 2015 in comparison to the 20th century base line. Based on data from NOAA (2020a) with permission from publisher NOAA.

to cooling in the respective time span (southern Patagonia). However, the overall trend, which is supported by temperature anomaly data (Fig 5b) shows an increase during the study period.

The precipitation data acquired from land-based weather stations around the world (Fig 6a) indicate a positive trend of global precipitation between 1989 and 2015. The NOAA data suggests an average rise of 2.03 mm per decade since 1901 (NOAA 2020b). A similar long-term trend was

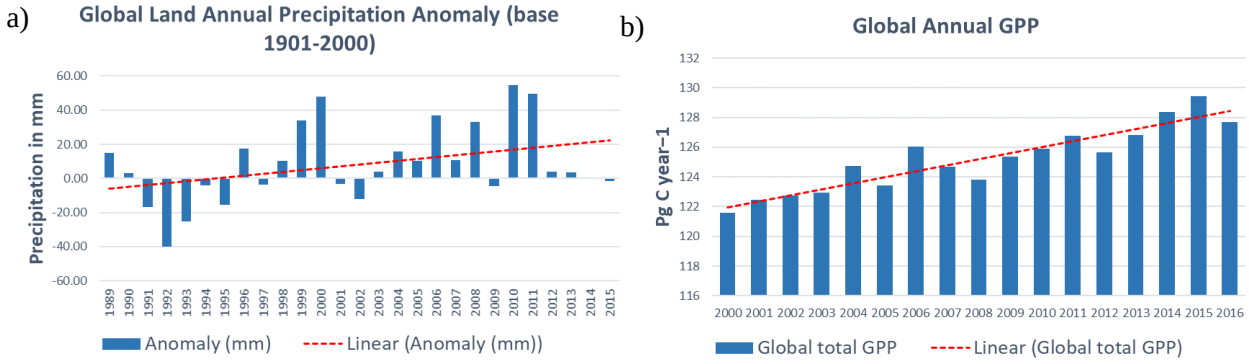

Figure 6 a) Global precipitation anomaly 1989 – 2015 Based on data from NOAA (2020b) with permission from publisher NOAA. b) Global annual GPP change between 2000 and 2016. Based on data from Zhang et al. (2017) permission from Yao Zhang.

concluded by the IPCC in 2013 but depending on the dataset with or without statistical significance (IPCC 2013). The increase is mainly due to more evaporation as a consequence of the temperature rise. Like temperature, the changes in precipitation are neither linear nor equally distributed. It is strongly dependent on regional or local conditions like wind patterns, ocean currents, vegetation, temperature, topography and ocean-atmosphere oscillations (Gebhardt et al. 2007).

The global gross primary production (GPP) (Fig 6b), a measure of carbon uptake (photosynthesis) by vegetation, shows an increasing global trend (Liu et al. 2015) with a total rise of about 4 petagrams carbon (in respect to the trend line (red), but with large annual variations) between 2000 and 2016 (Zhang et al. 2017). Note that GPP estimates are based on different methods. Therefore, the numbers vary depending on the method and data used. The estimate by Zhang et al. (2017) is based on MODIS data and light use efficiency theory. The result is in line with current research, suggesting higher atmospheric CO_2 concentrations lead to greater uptake of carbon by, and increased growth of, most plants due to increased photosynthesis (Taub 2010). Greening trends, expressed by NDVI, also correlate with increasing temperature in many regions, negatively in boreal forests, and positively in high northern latitudes and the Sahel Zone, but also correlations with precipitation were found, for example in China and the United States (Liu et al. 2015). The shown data point in a direction of global overall, but spatially variated increased NDVI, due to warming, higher atmospheric CO_2, and more total precipitation over the study period. A study by Pei et al. (2019) analyzed the relationship between NDVIg3 and climate indicators and found a significant (Pearson) correlation for temperature and precipitation for the study area. Several other regional (Ji and Peters 2004; Ding et al. 2007) and global (Kawabata et al. 2001; Ichii et al. 2002) studies scrutinized this relationship. But it is recognized that both time scales, the choice of NDVI analysis methods like the annual max NDVI, the inter-growing season and within-growing season method influence the relationship between vegetation and climate, which is found to be complex and nonlinear (Pei et al. 2019).

2.7 Environmental impacts measured by remote sensing instruments

Remote sensing is widely used by the military to monitor conflicts but also increasingly to observe their environmental impacts (Witmer 2015). A study on remotely assessed environmental impacts of war by Al Ajmi (2009) explains some applications used to measure the environmental effects of the Gulf War in Kuwait in 1991. Using satellite images captured by different sensors during the

war, environmental consequences like oil lake development and oil polluted surfaces were analyzed in post-war studies. The applications vary strongly and range from land surface temperature measurements for oil lake detection (thermal infra-red, Landsat TM band 6), post-war precipitation pattern change (visible, infrared and microwave, TRMM), palm tree detection for agriculture damage assessment (very high resolution (0.6 m) images, Quickbird), radar interferometry and elevation mapping to monitor post war production facility expansion (Synthetic Aperture Radar (SAR), ERS-1) and measuring of land-use, landcover, runoff, evaporation and evapotranspiration to assess water scarcity (Landsat ETM, TRMM, SRTM) (Al Ajmi 2009).

2.8 Measuring vegetation

Vegetation Indices (VI) correlate with other vegetation estimates like leaf area index (LAI) and aboveground biomass (AGB) production (Liang and Wang 2020b; Zhu and Liu 2015), therefore remote sensing data can be used to estimate vegetation status on a wide scale. However, the relationships can vary by region. For NDVI and aboveground productivity for instance their linear relationship can change due to the saturation effect in highly vegetated areas, leading to a declining relationship (Box et al. 1989). On the other hand in sparse vegetated areas, the soil background can disturb the signal, making it difficult to estimate the vegetation accurately (Huete 1988). The enhanced vegetation index (EVI) was created to overcome the saturation effect (Levy 2000) but cannot be used with AVHRR sensors since it is lacking the blue band. Hence, due to the long-term scope of this study, NDVI is the best option.

Two of AVHRRs detectors are observing light in the spectra between 0.58 – 0.68 μm (visible light = 0.38 – 0.75 μm) and 0.725 – 1.10 μm (NIR = 0.76 – 1.5 μm) respectively (Al Ajmi 2009; Shimabukuro et al. 1997). Hence, the detectors can identify differences of surface types and even varying vegetation types based on their spectral reflectance. Healthy vegetation absorbs most of the visible light, especially in red and blue wavelengths regions of the electromagnetic spectrum and reflects most of the NIR light. The light is trapped in the chlorophyll pigments inside the leaves and the energy used by plants for photosynthesis. The discovery of this spectral ratio, in the late 1960s led to the development of VI's using this ratio to discriminate green vegetation from soil and other land cover types (Tucker 1979). Different land cover types, and even broad categorizations of vegetation like shrubs, desert and tropical forests can be differentiated.

For large scale vegetation analysis, composites are useful products for spatial consistency and cloud-free images. For the Global Inventory Modeling and Mapping Studies (GIMMS) dataset daily imagery were converted to NDVI scenes, and then on a pixel by pixel basis compared and the maximum values retained. This so called maximum-value composite procedure (MVC) reduces common remote sensing error sources like aerosol and water-vapor effects, directional reflectance, sun angle, shadow and off-nadir viewing effects (Holben 1986). On the downside, it is assumed that these effects reduce the spectral signals and therefore the NDVI value. To reduce these non-vegetational attenuations the daily data is filtered to select maximum pixel values. Another downside of the MVC technique is the generalization of the daily NDVIs for the period to one value, which represents the vegetation response for this time. Depending on the response time of the particular vegetation and the length of the growing season, a too long time interval for the image composites reduces the accuracy of the response curve. Or in other words if the period for combining the data exceeds changes in the response curve, there cannot be any conclusions drawn for the vegetation response (Holben 1986). In regions with long growing seasons, like the tropics, longer periods for the composites can be used, to still be able to draw conclusions of the phenology and have the advantage of longer MVCs to reduce cloud noise etc. For global coverage, 16-day composites, using daily AVHRR scenes are found to be a useful compromise.

GIMMS data is widely used for long term NDVI trend analysis (Guo et al. 2017). Even though studies based on satellite data did result in varying NDVI trends (Beck and Goetz 2011), the long time span makes the GIMMS dataset an important source for analysis of vegetation and climate variability. A quality assessment of the third generation GIMMS dataset 'NDVIg3' was conducted by (Kern et al. 2016) in comparison to MODIS data for central Europe. The authors conclude that especially on regional scale, the dataset shows strong discrepancies with MODIS NDVI data. Nevertheless, on global scale, and for long-term studies the dataset provides valuable information, for which reason it was widely used for analyzing vegetation trends and dynamics (Kern et al. 2016).

3 Study area

There is no predefined spatial exclusion of regions for this study. Therefore, it is essentially a global analysis. However, since only areas with conflict events between 1989 and 2015 will be included, the spatial focus will be on certain areas. Most conflicts occurred in Equatorial Africa,

parts of the Middle East, Central America and the northern states of South America, the Sahel Region, the Balkan Region, parts of South East Asia and parts of Central Asia. However, to answer question one, two and four, global datasets will be used, without any regional filter. For visualization purposes, the results of question one will be displayed regionally instead of globally. Note that the regions for this chapter are subdivided according to UCDPs territories in Africa, the Americas, Asia, Europe and the Middle East. All conflicts in this section are positioned between Lat 47N and -30S. For question 3, the focus is on Rwanda and Afghanistan to analyze the data on a larger scale and for specific armed conflicts, which are defined as intrastate conflict and intrastate conflict with foreign involvement (UCDP 2019) respectively. Afghanistan is located in the Middle East, with arid to semi-arid climate, and low NDVI values (mean value of 0.20 in the conflict zones) and Rwanda is a small eastern African country characterized by high precipitation, high temperatures and NDVIs averaging at 0.68. These two conflicts were chosen, mainly due to these climatic and vegetation differences, representing extreme arid and extreme wet areas. Additionally both conflicts occurred during the period of considered conflicts (1989 – 2009).

As visible in figure 7 the main areas analyzed are located in the tropical zone. Note that values below 0 (light blue) represent excluded pixels (see chapter 4.2.1). These data points are especially prominent in areas with low (<0.2) and very high (>0.8) surrounding NDVI values, for example in arid regions in Central Australia and Saudi-Arabia, or in dense tropical forests like in Equatorial Africa, the Amazon and Indonesia (Fig 7).

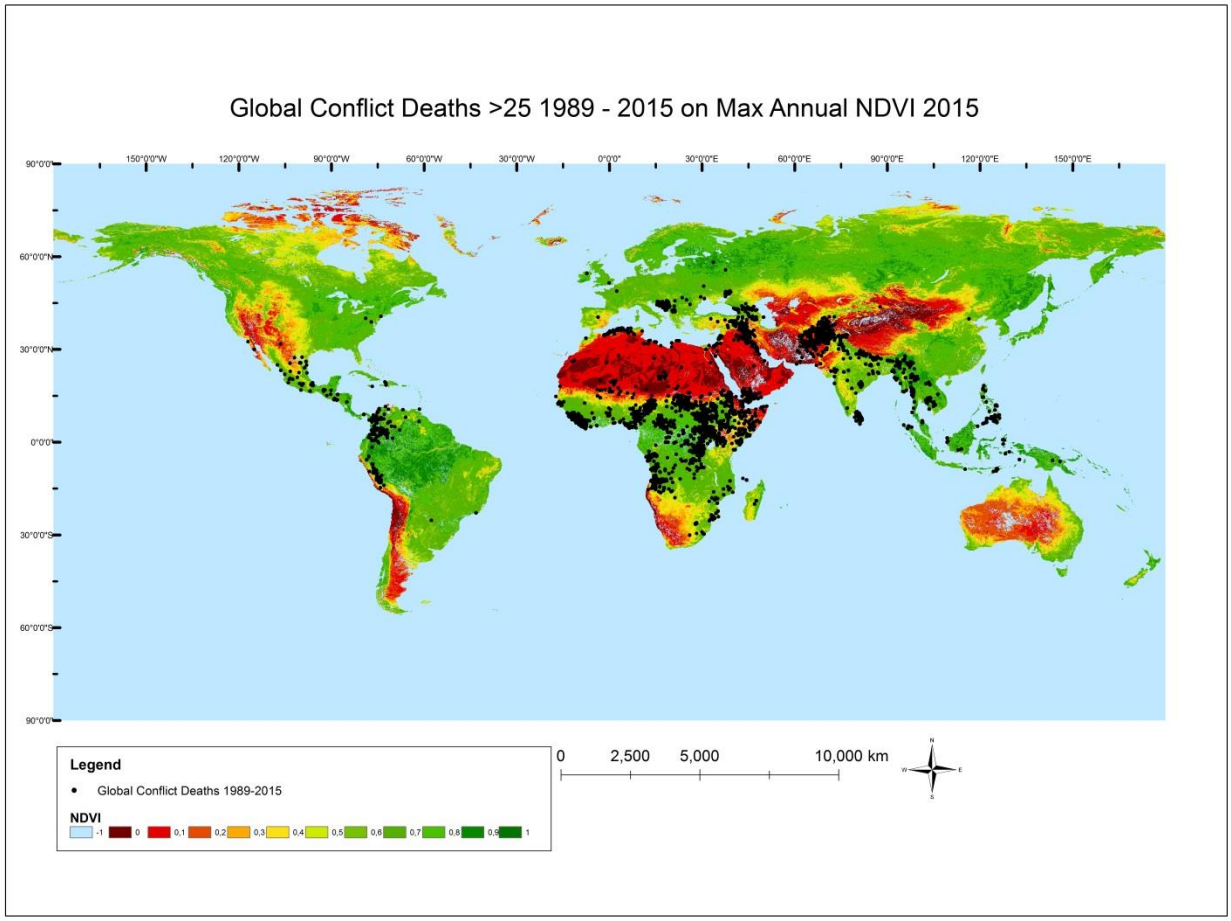

Figure 7 Global distribution of conflict events (best estimate) with more than 25 deaths (black dots), displayed on a global NDVI annual maximum map for 2015. Based on data from UCDP (2020a) and Tagesson & Tian 2020 permission from Torbern Tagesson and UCDP.

4 Materials and methods

4.1 Data description

For the analysis, three datasets, georeferenced conflict data, global NDVI data and climate data, are used, which will be described further in the next sections.

4.1.1 Conflicts

Information about worldwide conflicts are accessed through the 'UCDP Georeferenced Event Dataset (GED) Global version 19.1', which is available at the website of the Uppsala Conflict Data Program (UCDP) located at the Department of Peace and Conflict Research, at Uppsala University (UCDP 2020a). In this dataset global conflict data ranging from 1989 to 2018 (excluding Syria) is available (Sundberg and Melander 2013a). For this study the data is reduced to the columns 'year', 'type_of_violence', 'latitude', 'longitude', 'geom_wkt' , 'region', 'country' and 'deaths', and to the years 1989 to 2015. All events are georeferenced according to the World Geodetic System of 1984 (WGS 84) (Högbladh 2020). For the column 'type_of_violence' the data is divided into type: 1) state-based conflict, 2) non-state conflict and 3) one-sided conflict. The regions are grouped into Africa, Americas, Asia, Europe and the Middle East. For the event death number titled 'deaths', the 'best estimate' is used. Low and high estimates are available as well, which might be appropriate for other studies.

The UCDP data is based on three types of sources: "global newswire reporting", "global monitoring and translation of local news performed by the BBC" and "secondary sources such as local media, NGO and IGO reports, field reports, books etc." (Högbladh 2020, p.12). The data is collected and provided by Dow Jones Factiva, a digital archive of global news content. International newspapers like Reuters News, Agence France Presse or BBC Monitoring are monitored and the content filtered by key words such as 'kill', 'die' 'injure', 'dead' or 'death' (Högbladh 2020, p.12). Note, that in all UCDP databases the sources are specified in the 'source_article' variable, but since there is no evaluation of the sources, for example to consider media consistency, which can be useful for some studies, this variable is excluded. By using several different sources to collect the data from, flexibility in reacting on inconsistencies in the news coverage of the organizations is guaranteed, for example if managerial focuses or organizational structures change.

The data is filtered to only include events with at least one casualty in the 'best estimate' category. This means if sources report differing death numbers, which are listed as 'high estimate' or 'low estimate' a best estimate depending on the trustfulness of the sources is made to conclude on the most reliable death number. Note, that events with no deaths, or an unclear number of deaths for all three estimate categories are excluded in the UCDP datasets (Sundberg and Melander 2013a).

The georeferenced UCDP conflict data is filtered according to the conflict study period (1989 – 2009) and the categories, relevant for the analysis of the four aims. For aim 1-3), data is filtered to consist of events with at least 25 deaths, in order to avoid minor incidents. This threshold is firstly based on the assumption that larger events, in terms of their death number, are more likely to lead to so called 'visual manifestation'. Meaning they have a higher chance to directly or indirectly impact their surroundings, and secondly the 25 deaths threshold is used by UCDP to define armed conflicts for all three conflict types. Additionally, the data is separated by, conflict types 1) state-based conflict, 2) non-state conflict, 3) one-sided violence for aim 2 (Högbladh 2020); the data for Rwanda and Afghanistan is extracted for aim 3; and by casualty numbers 1) more than zero, 2) more than 25, 3) more than 100 for aim 4. Note that for Afghanistan it will be focused on the first two (out of three) phases of the Afghanistan War, which are mainly characterized by the 2001 US response to 9/11 (phase one), and the 2002-2008 NATO-Taliban War (phase two) (Witte 2018). This war resulted in 27844 deaths in 3749 events between 2001 and 2008, according to UCDPs GED dataset. For Rwanda only events occurring during the genocide in 1994 are included.

4.1.2 NDVI

The GIMMS NDVI image collection, used for this project, is provided by NOAA and is measured by AVHRR sensors onboard NOAA's 7, 9, 11, 14, 16 and 17 satellites. The images are corrected and calibrated for stratospheric volcanic aerosols, orbital drift and viewing geometry (Tucker et al. 2005). The bi-monthly composites are available from 1981-07-01 to 2015-12-31 with a spatial resolution of 1/12-degree (8 km equal area). Note that the GIMMS NDVI3g dataset is only available until 2013-12-31 in GEE and since, in this study, long-term trends are subject of interest and seasonal variations needed to be excluded, it is decided to use an annual maxima dataset until 2015-12-31 instead (see chapter 4.2.1.2).

4.1.3 Climate

The TerraClimate ~4 km spatial resolution, global terrestrial surface dataset consists of 14 bands mainly for climate and water balance variables for the period 1958 to 2019 and is annually updated.

Table 1 Climate variables overview Based on data from Abatzoglou et al. (2017) permission from GEE (public domain).

Name	Units	Min	Max	Scale	Description
tmmx	°C	-670	576	0.1	Maximum temperature
pr	mm	0	7245		Precipitation accumulation
soil	mm	0	8882	0.1	Soil moisture

It combines the climate data from the WorldClim dataset with other datasets such as the CRU Ts4.0 (Harris et al. 2014) and the Japanese 55-year Reanalysis (JRA55) (Kobayashi et al. 2015) to produce an interpolation-based global climate and water balance dataset (Abatzoglou et al. 2018). By applying the water balance model, hydrological variables such as precipitation, evapotranspiration, and soil water capacity are added.

The TerraClimate temperature (T) and precipitation (P) data is acquired from the WorldClim v1.4 and v2.0 datasets, which consist of measurements from thousands of weather stations (Hijmans et al. 2005). The datasets are modified by the CRU Ts4.0 and the JRA-55 to create monthly maximum temperature (tmmx) ranging from -67.0°C to 57.6°C (Table 1) (Abatzoglou et al. 2017).

For P the maximum value of the monthly accumulated precipitation band 'pr' from TerraClimate ranging from 0 to 7245 mm is used. The soil moisture (SM) is based on a simple Thornthwaite water balance model and satellite based estimates to extract soil water storage capacity data at a 0.5° grid (Abatzoglou et al. 2018; Wang-Erlandsson et al.

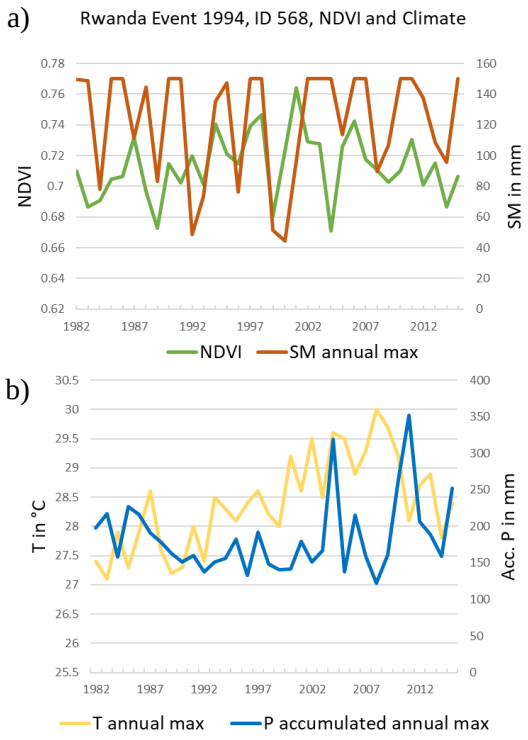

Figure 8 Comparison of: a) annual maximum NDVI and soil moisture (SM annual max), and b) annual maximum temperature (T annual max) and annual maximum of monthly accumulated precipitation (P accumulated annual max). The one-sided violence event occurred in eastern Rwanda in 1994 and led to 22 deaths. Based on data from UCDP (2020a) and Tagesson & Tian 2020 permission from Torbern Tagesson and UCDP.

2016). For many conflict regions the annual SM values stay constant over parts of, or for the full study period (Fig 8a).

For an impression of the data see figure 8 which displays a randomly picked conflict (pixel) in eastern Rwanda in 1994 and the according NDVI and climate variables over the study period.

4.2 Analysis

4.2.1 Data preparation

4.2.1.1 NDVI

For the smoothing and gap-filling of the NDVI time series, a double logistic fitting method is used with the TIMESAT software (Jönsson and Eklundh 2004). The double logistic method smooths seasonality curves around maxima and minima, have a low sensitivity to noise and it is therefore reported to perform best on time series without a well-known quality (Beck et al. 2006; Jönsson and Eklundh 2004; Zeng et al. 2011). The parameters applied in TIMESAT are: seasonal parameter = 0.5, number of envelope iterations = 2, adaptation strength = 2, Savitzky–Golay window size = 4, start of growing season = 0.2, end of growing season = 0.2. To remove outliers from the NDVI time series, a median filter spike method is used with the spike parameter set to 2.0. From these TIMESAT smoothed time series, the annual maximum of NDVI are extracted representing amount of green vegetation (Tagesson et al. 2016).

The conflict datasets consisting low quality flagged NDVI values are excluded from the analysis. The conflict datasets inheriting such values in any year, are excluded from the analysis, since an equal time period before and after the conflict is necessary.

Table 2 Comparison of the 8 datasets, subdivided by the aims and sub-aims. Note that Aim 1 and Aim 4b are the same. Based on data from UCDP (2020a).

		Data Desctiptor	Death Threshhold	Number of Events	Number of NDVI values	Min.	Max.	Mean	Std. Dev.
Aim 1		All	>=25	6038	205292	0.0011	0.9991	0.5802	0.2388
Aim 2	a)	Type 1	>=25	3897	132498	0.0012	0.9991	0.5508	0.2428
	b)	Type 2	>=25	774	26316	0.0740	0.9930	0.5766	0.2258
	c)	Type 3	>=25	1367	46478	0.0516	0.9991	0.6682	0.2106
Aim 3	a)	Afghanistan	>=25	203	6902	0.0734	0.5676	0.2008	0.0885
	b)	Rwanda	>=25	249	8466	0.5127	0.8817	0.6783	0.0508
Aim 4	a)	Threshhold 1	>=1	30840	1048575	0.0029	0.9995	0.5862	0.2466
	b)	Threshhold 2	>=25	6038	205292	0.0011	0.9991	0.5802	0.2388
	c)	Threshhold 3	>=100	1483	50422	0.0012	0.9853	0.5900	0.2309

Eight datasets are created in GEE to address the 4 aims of this study (Table 2). Aim 1 and aim 4b uses the same dataset. Aim 1 data is used again in aim 4 to enhance differences and to compare

and visualize the deaths greater 25 dataset against the other two death threshold datasets (>0 and >100). Each dataset consists of NDVI and climate data for each conflict for the period between 1982 and 2015. Additionally, the 'slopeYears', and other descriptive information is added to each conflict, in separate columns. As expected, the statistical indicators of the global datasets, even if varying in size (number of events and NDVI values) are similar to each other. All of them contain high maximum NDVI values (>0.9853) and low minimum NDVI values (between 0.0011 and 0.0740). The same similarity counts for the standard deviation (Std. Dev.), ranging between 0.2106 and 0.2466. The regional datasets show the lowest and the highest average NDVIs, with 0.2008 (Afghanistan) and 0.6783 (Rwanda) respectively.

4.2.1.2 Climate

Since the focus is on long-term trends, the monthly climate data, needs to be converted into annual values. Therefore, a maximum annual climate image collection is generated in GEE by extracting the TerraClimate image collection data using a pixel by pixel comparison of the monthly maximum T, monthly accumulated P and SM values, after filtering for the study period and study area. Note, the spatial resolution is ~4 km, whereas the GIMMS dataset is 8 km. The pixels are not aligned accurately to each other. Meaning that TerraClimate pixels are often not limited to the area of GIMMS pixels, due to the random position of the conflict inside the pixels. Nevertheless, both datasets are of coarse spatial resolution, with pixels covering large areas, and it will not be focused on single pixels and single NDVI values but rather the trends over large areas.

4.2.2 Impact of conflicts on vegetation greenness on global scale

To analyze the effects of conflicts on vegetation, the change in NDVI between the periods before and after the events will be compared. Hence, the effect of the events is calculated by comparing NDVI for a period of at least six years and up to 17 years after each event to the period with the same length before the event. The minimum period of six years is based on a trade-off between 1) not excluding too many events in the beginning and end of the time-series, and 2) to keep a long enough period to get accurate trend estimations. This excludes conflicts occurring before 1987 and after 2010. However, since the UCDP database starts in 1989, the lower filter is only theoretical. A first script in GEE extracts the NDVI values and the length of the periods for the conflict locations. In the same manner, the annual TerraClimate data is also extracted for the conflict locations.

Next, trends are estimated by fitting ordinary least square regressions with the NDVI values as dependent variable to their respective years as independent variable. Hence, two slopes per conflict, for the periods before (slope_BC) and after (slope_AC) the conflicts are extracted. Next these slope estimates are subtracted from each other. They are named 'AC-BC' and are interpreted as proxies for changes in the trends before and after the conflict. In addition, mean values of NDVI and climate (T, P, SM) are calculated for every conflict for both periods.

4.2.2.1 Producing climate-controlled slopes

Since climate variability over the study period of 34 years is likely to affect vegetation, and therefore observed NDVI (Ichii et al. 2002; Schultz and Halpert 1993), a model is used to control for this influence. A multiple linear regression is fitted with NDVI values as dependent variable and climate (T, P, SM) as independent variables for the period before every conflict:

NDVI_CC = (Intercept) + T(BC)*Coef_1 + P(BC)*Coef_2 + SM(BC)*Coef_3

This regression is used as a predictive model to generate the climate controlled (CC) NDVI for the after conflict period. Hereinafter named (CC) in contrast to NDVI observed values for the AC period which are named (AC) for simplification. Next, trends are estimated by fitting ordinary least square regressions with the CC values as dependent variable to their respective years as independent variables. Then the impact of climate on the trend changes is calculated as the slope_CC subtracted from the slope_BC (CC-BC). Note that a lot of missing values were found and since the conflict data tables involving missing data in any of the four variables are filtered out, a large number of conflicts is excluded in the CC analysis. Therefore, the CC analysis, is based on a much smaller dataset (2729) in comparison to before conflict (BC) dataset (4429), leading to changed NDVI CC statistics.

Lastly, summary statistics namely medians, means, standard deviations, minima, maxima and first and third quartiles are calculated to get overall proxies for the changes of the trends. To scrutinize the climate variability further, means of NDVI, T, P and SM for both periods before and after each conflict are calculated. These are then subtracted to assess their difference.

4.2.3 Effects of different types of conflicts on vegetation greenness

To analyze the effect of different types of conflicts on greening the input conflict data for the regression analysis, is adjusted as described in chapter 4.1.1. Hence, conflicts with more than 25 deaths are included and the datasets are filtered according to the three conflicts types: state-based violence, non-state violence and one-sided violence. The visualization of the output data will be concentrated on enhancing the differences between the conflict types. For that, boxplots are created for each conflict type for both AC-BC and CC-BC. In addition, to compare NDVI directly, mean NDVI differences are calculated for AC-BC and CC-BC and are also plotted in a boxplot.

4.2.4 Comparison of the Rwanda genocide and the Afghanistan War

For the conflict examples the input data is filtered according to the description in 4.1.1. Therefore, only conflicts occurring in Rwanda and Afghanistan are considered. The death threshold is again >25 in this analysis. Most of the events are filtered out due to this threshold, resulting in 203 events for Afghanistan and 249 events for Rwanda. Boxplots are created for AC-BC and CC-BC slope differences. Additionally, the conflict locations are projected on two regional maps to show the spatial distribution. Note that for Rwanda only data of one year (1994) is used, so the slope periods are all the same.

4.2.5 Effect of fatality number, extend of event

Similar to chapter 4.2.3 the analysis for the effect of the fatality number of conflicts on NDVI mainly differs by the input dataset used. To address this aim the input data is filtered as described in the data description chapter 4.1.1, according to their death thresholds: >0, >25 and >100. Boxplots are created for AC-BC and CC-BC for both the slope differences and the NDVI means differences.

5 Results

5.1 Impact of conflicts on vegetation greenness on global scale

The main results for the global analysis are listed in table 3. The NDVI means after the conflicts are slightly higher compared to before the conflicts. In contrast the NDVI slopes decreased but are still positive. However, these changes are insignificantly low. Note that the sample size is smaller due to the missing data in the climate and NDVI datasets and that they differ between the results.

The aggregate functions show the distribution of every dataset, in terms of their extrema (Min & Max), tendencies (Median & Mean) and spread (1st Qu., 3rd Qu., & Std. Dev.)

Table 3 Global analysis statistical overview. 'BC / AC' represents observed NDVI for both periods and 'BC / CC' observed NDVI for before conflict and predicted NDVI for after the conflicts. For both parts statistics on NDVI means, slopes and the subtractions of both for every considered conflict is shown. Note, NDVI is given in a range between -1 and 1. Both parts of the data table list aggregate functions like minimum, first quartile (median of the lower half of the dataset), median, mean, third quartile (median of the upper half of the dataset), maximum and standard deviation (Std. Dev.).

Aim 1		Min	1st Qu.	Median	3rd Qu.	Mean	Std. Dev.	Max.
BC / AC	mean NDVI before	0.0225	0.3945	0.6389	0.7500	0.5718	0.2273	0.9643
	mean NDVI after	0.0268	0.3976	0.6486	0.7554	0.5798	0.2289	0.9648
	slope before	-0.0472	-0.0014	0.0022	0.0059	0.0027	0.0096	0.0957
	slope after	-0.2270	-0.0028	0.0011	0.0043	0.0009	0.0101	0.0553
	differences in NDVI	-0.1078	-0.0005	0.0099	0.0240	0.0118	0.0222	0.1306
	differences in Slopes	-0.2652	-0.0069	-0.0012	0.0040	-0.0018	0.0131	0.0633
BC / CC	mean NDVI before	0.0225	0.3945	0.6389	0.7500	0.5718	0.2273	0.9643
	mean NDVI after	-0.2813	0.3018	0.5336	0.6793	0.4925	0.2224	0.9930
	slope before	-0.0472	-0.0014	0.0022	0.0059	0.0027	0.0096	0.0957
	slope after	-0.2284	-0.0050	0.0004	0.0057	0.0003	0.0219	0.2585
	differences in NDVI	-0.2374	-0.0042	0.0015	0.0098	0.0026	0.0243	0.3360
	differences in Slopes	-0.2301	-0.0085	-0.0019	0.0044	-0.0024	0.0251	0.2655

Median and mean NDVI are higher after the conflicts ($0.6389 < 0.6486$ and $0.5718 < 0.5798$), whereas the mean and median for the slopes are lower after the conflicts ($0.0022 > 0.0011$ and $0.0027 > 0.0009$). In other words, the NDVI values on average are higher after the conflicts, but the change in NDVI (represented by the slopes) is lower, but still positive. This can additionally be seen by looking at the differences. They are positive for NDVI means (0.0099 and 0.0118) but the trends are slightly negative (-0.0012 and -0.0018). However, the spread indicators depict a relatively strong variance of the data, with many NDVIs and slopes pointing in the reversed direction as the mean values. For example, the standard deviations (supported by the 1st and 3rd quartiles) for 'differences in NDVI' (0.0222) and 'differences in Slopes' (0.0131) compared to their means (0.0118 and -0.0018), shows that a large portion of the NDVI means are lower or higher respectively, in the AC period compared to the BC period.

By visually scrutinizing the global distribution of positive and negative slope changes using the 'AC-BC' dataset (Fig 9), some distinctive spatial features and regional differences can be identified. In Africa (Fig 9a) a large number of conflicts are in or below the Sahel Zone, with a majority of conflicts in Eastern Africa. No distinctive difference in the spatial distribution between pos. and neg. slope changes are visible for this region. The same counts for Asia (Fig 9c). In the Americas, Europe and the Middle East (Fig 9b/d/e respectively) some places show a

disproportional spread of either positive (Peru, central Iraq) or negative (southeastern Europe, Armenia, Azerbaijan and its border region with Russia) slope changes.

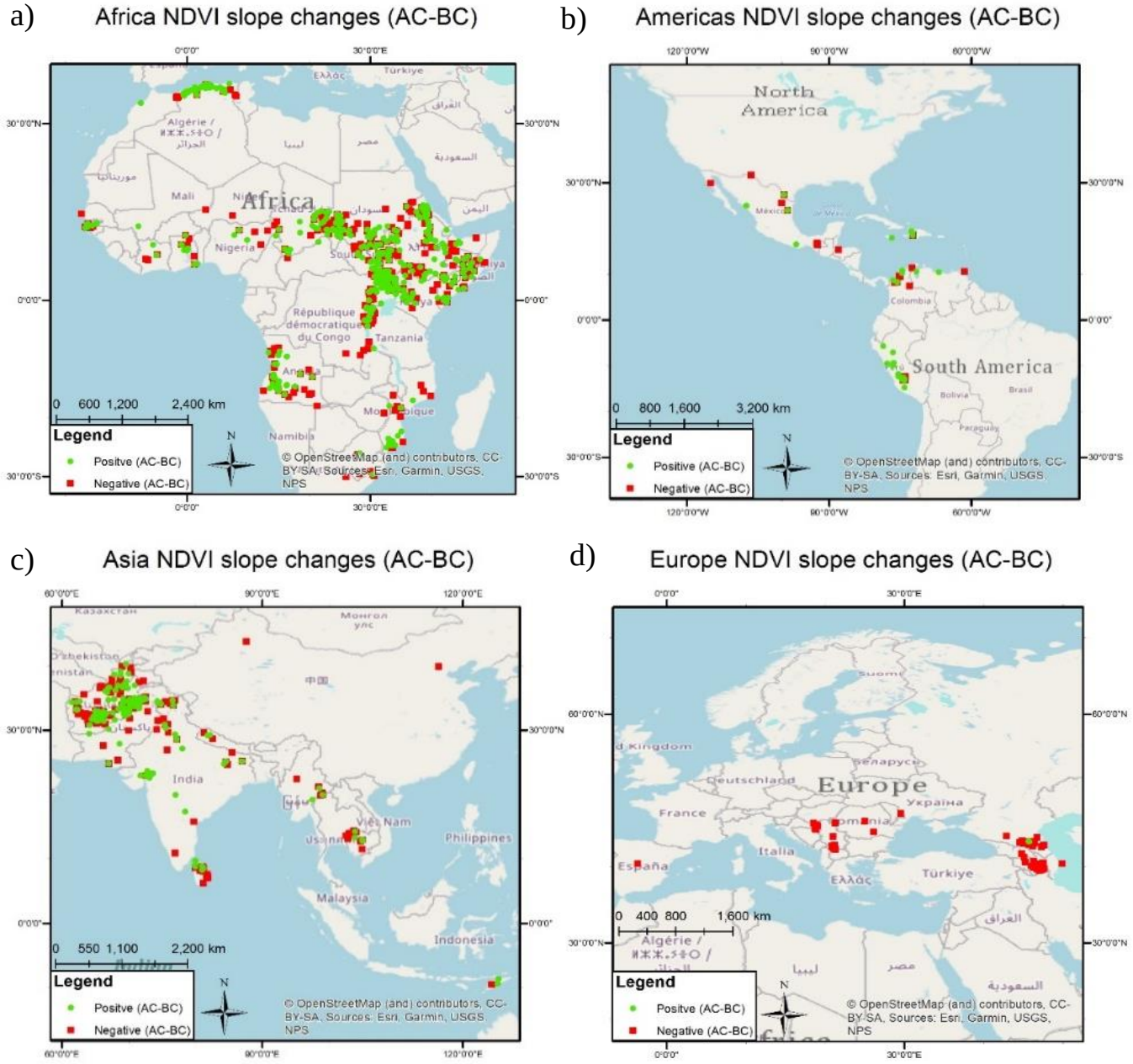

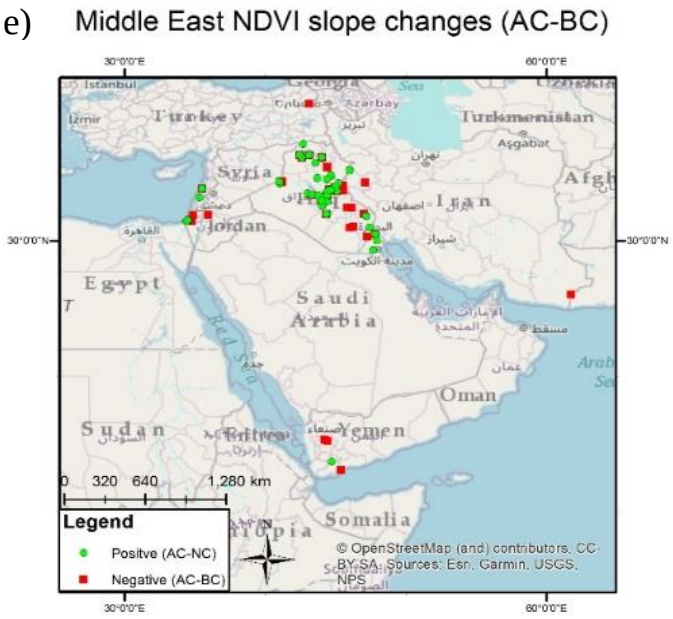

Figure 9 Global distribution of slope changes (AC-BC) subdivided into regions, based on USDPs division. Conflicts (>25 deaths) locations are positive trend changes (green circles) and negative trend changes (red squares) are estimated. a) Africa, b) Americas, c) Asia, d) Europe and e) Middle East. The maps focus on the datapoints, and therefore areas with no conflicts are in some cases outside the window. Based on data (conflict locations) from UCDP (2020a).

5.1.1 Impact of climate on NDVI before and after the conflict

Comparing the findings of the upper part of table 3 to the CC statistics (lower part of table 3), it gets evident that the climate based NDVI values are mainly lower than the observed ones. The mean CC_NDVI is 0.4925 compared to the AC mean with 0.5798, which is a reduction of 0.0873. Additionally, on average the slopes for CC are positive but much lower compared to AC. Alike AC the general tendency for slope changes is negative, and due to the lower CC slopes, the

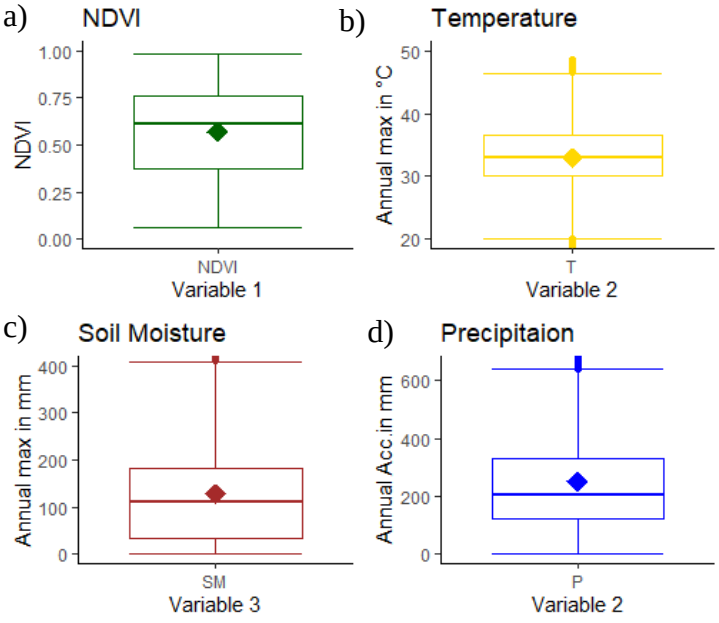

Figure 10 Comparison of distribution of input a) NDVI, b) temperature, c) soil moisture and d) precipitation data. The colored dots represent the mean and the line inside the boxes the median.

differences are slightly bigger.The comparison of input NDVI to the three climate variables T, SM and P (Fig 10) using boxplots shows that the Interquartile Range (IQR) of the NDVI data is between ~0.75 and ~0.4, whereas the extrema are spread throughout the full NDVI range (only positive side), compared to an IQR of approx. 30 to ~37°C for T annual max, ~50 to almost 200 mm for annual max SM and ~110 to ~350 mm for annual max P. The spread of most values is therefore rather limited, whereas the extrema (upper and lower horizontal lines) display the large variations for all datasets, representing weighted global climate and vegetation datasets. 'Weighted', in terms of overrepresentation of some conflict regions and exclusion of the majority of countries without any conflicts in the past three decades. The means are greater than the medians in the SM and P datasets, meaning it is positively skewed, whereas the median is less for NDVI and T meaning a negative skewness of distributions. This is supported by the quartiles and extrema showing a large spread of values in the upper quartile for both SM and P and therefore the positive skewness. The temperature values are more equally distributed with a total range (excluding outliers) of about 20 to ~46°C.

A comparison between the mean differences in NDVI with the mean differences in climate variables, indicate strong positive relationships with both T and SM (Fig 11). In other words, with increasing differences in T and SM between AC and BC, the differences in mean NDVIs are increasing as well. Therefore, the increase in T and SM in these regions explain on average the

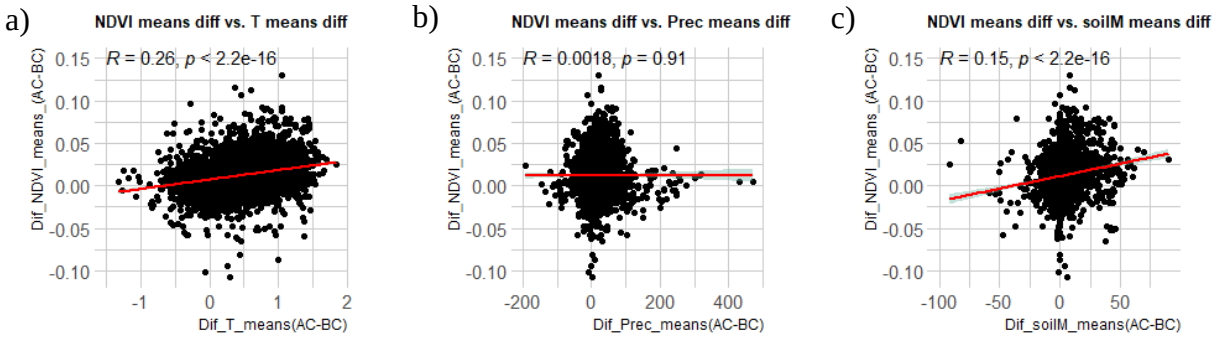

Figure 11 Difference in NDVI averages for every conflict against, a) difference in temperature means, b) difference in precipitation means, c) difference in soil moisture means. Note, every difference value is calculated by subtracting the mean for the full AC period for each conflict by the mean for the full BC period for every variable.

slight increase in NDVI_AC. The mean differences in T and SM are 0.42 and 1.89, respectively. The ordinary least square linear regressions (Fig 11) thereby indicate an average increase in NDVI of 0.01 as caused by temperature, and 0.0003 as caused by SM for the period after the conflict.

As shown in table 3, there is no statistically significant increase in NDVI for the AC versus BC periods, but the climate control resulted in much lower NDVI values.

To show an example of the effect on the slope changes for the global dataset on a regional level, in figure 12 a comparison of a map window (Burundi) is used. It clearly shows how the

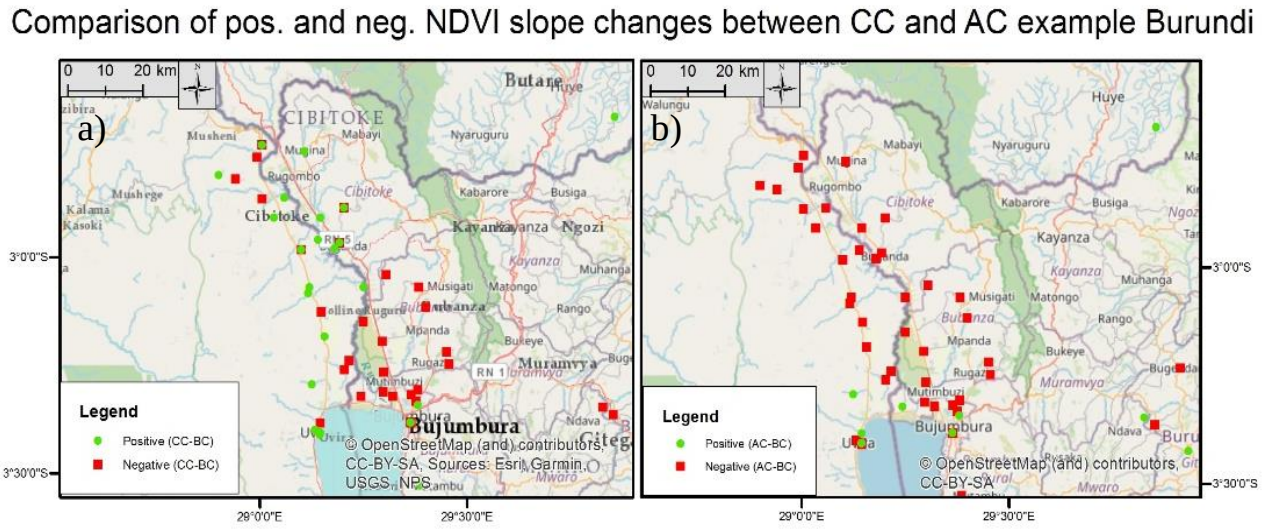

Figure 12 Spatial distribution of positive (green circles) and negative (red squares) NDVI trend changes for conflict locations included in the conflict deaths >25 dataset. a) climate controlled NDVI slopes differences (CC-BC) and b) comparison of observed NDVI slopes differences (AC-BC), both for Burundi (East Africa). Based on data (conflict locations) from UCDP (2020a).

climate effect altered the vegetation trends for some conflicts. In the northwestern boarder region of Burundi, and its neighbor the Democratic Republic of the Congo, the majority of observed (AC-BC) NDVI trend differences are negative (Fig 13b, red squares). When comparing them to the CC slope changes (Fig 12a) it can be seen that most of the dots change, even though the global-scale summary statistics didn't show strong differences in the trends.

5.2 Effects of different types of conflict on vegetation greenness

For comparability reasons the same statistics as for table 3 (Ch. 5.1) are utilized (with exception of the Std. Dev.) but they are displayed in boxplots for a better overview of the three types and for enhancing differences between observed (AC-BC) and climate controlled (CC-BC) results.

On average the three main conflict types, 'state-based violence', 'non-state violence' and 'one-sided violence', all have negative tendencies, with both median and mean being slightly negative. Only the non-state conflict type shows a positive mean. However, it also inherits the greatest interquartile range, and a negative median, meaning that most of the slopes are negative, but some large positive slope values (outliers are not displayed but included in calculation) leading to a positive mean.

However, it can also be seen that for every dataset, there are large numbers of values on both

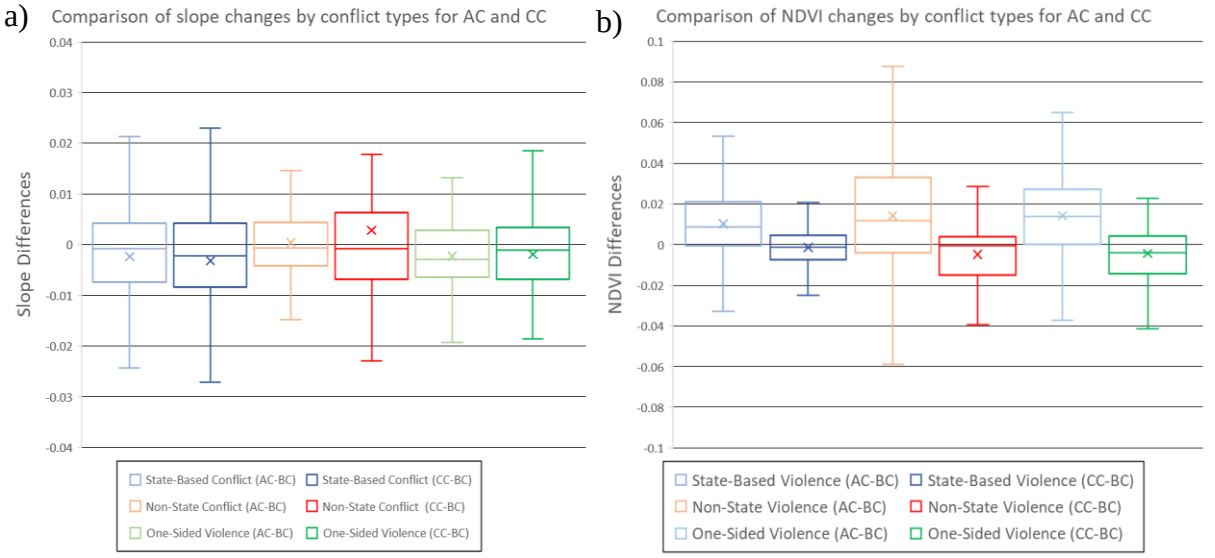

Figure 13 Comparison of a) slope changes and b) NDVI changes, for three conflict types. The datasets include all global conflicts >25 deaths for the study period. For each type, both, observed (dull colors = AC-BC) and climate controlled (richer colors = CC-BC) are shown. Note that the types are called both violence and conflicts, but they mean the same.

sides of the x-axis, meaning there are no significant positive or negative trends observable for any conflict type. Nevertheless, looking only at the observed slopes, the conflicts defined as one sided violence tend to have a stronger negative impact, than the other two types, whereas the state-based conflicts tend to have a larger impact considering only CC change slopes.

Looking at the plots in figure 13b much more variation between observed and predicted (CC) values can be observed. Medians and means are generally higher and ranges for extrema and interquartile range larger for observed NDVI changes than for predicted ones. All three AC datasets have positive tendencies, meaning generally higher NDVI values in the after-conflict period, whereas the CC values tend be below 0. Interestingly in contrast to the slopes, almost all observed NDVI changes are positive with only the lower whiskers reaching into negative areas, with exception for some non-state violence locations, which lower quartile shows some negative difference values. In conclusion, separating the dataset into the three main conflict types, is not resulting in significant varying impacts of conflicts on neither mean NDVI nor trends in NDVI. Only slight tendencies are found.

5.3 Comparison of the Rwanda genocide and the Afghanistan War

For Afghanistan the observed values are distributed in an almost standard distribution shape around zero with the first and third quartiles being between 0.01 and -0.01 (Fig 14). No significant difference in trends can be observed for the Afghanistan dataset.

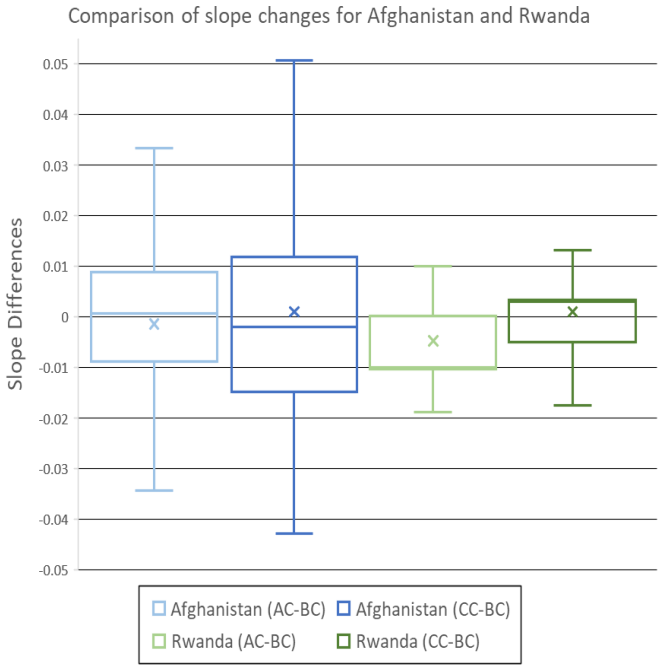

Figure 14 Comparison of slope changes for Afghanistan (blue) and Rwanda (green). The datasets include all global conflicts >25 deaths for the periods of the armed conflicts. For each example both, observed (dull colors = AC-BC) and climate controlled (richer colors = CC-BC) are shown.

The observed Rwanda dataset shows a negative tendency. However, the median is almost the same as the lower quartile. This is due to an agglomeration of the same slope values (~ -0.01) appearing several times. Hence, if we assume a similar NDVI development for Rwanda, which is likely due to its relative homogenous vegetation (Std. Dev. of input NDVI = 0.0508, Table 1), and small country size, the slopes are expected to be similar. The negative tendency in Rwanda is also observable in the Rwanda overview map (Fig 15b) where negative slopes are abundant and almost no positive trends are visible.

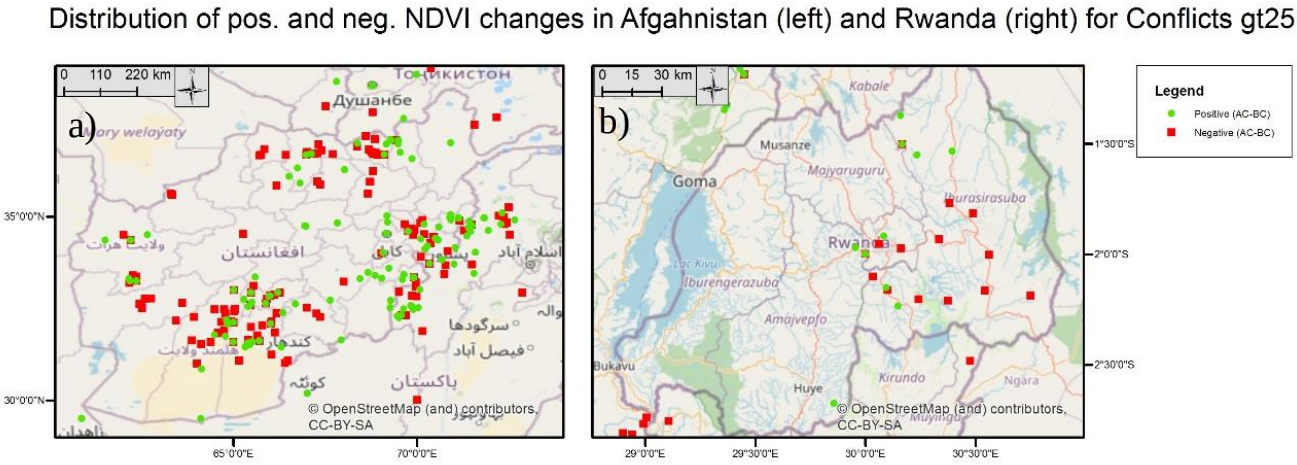

Figure 15 Spatial distribution of positive (green dots) and negative (red dots) NDVI trends for conflict regions included in the conflict deaths >25 dataset for a) Afghanistan and b) Rwanda. Based on data (conflict locations) from UCDP (2020a).

5.4 Effect of fatality number, extend of event

The fatality number, meaning the number of people who died, on average, per conflict event, seems to have an inisgnificant impact on the slopes and NDVI values. Only marginal differences between the slope datasets are present (Fig 16a). Nevertheless, considering the slope indicators,

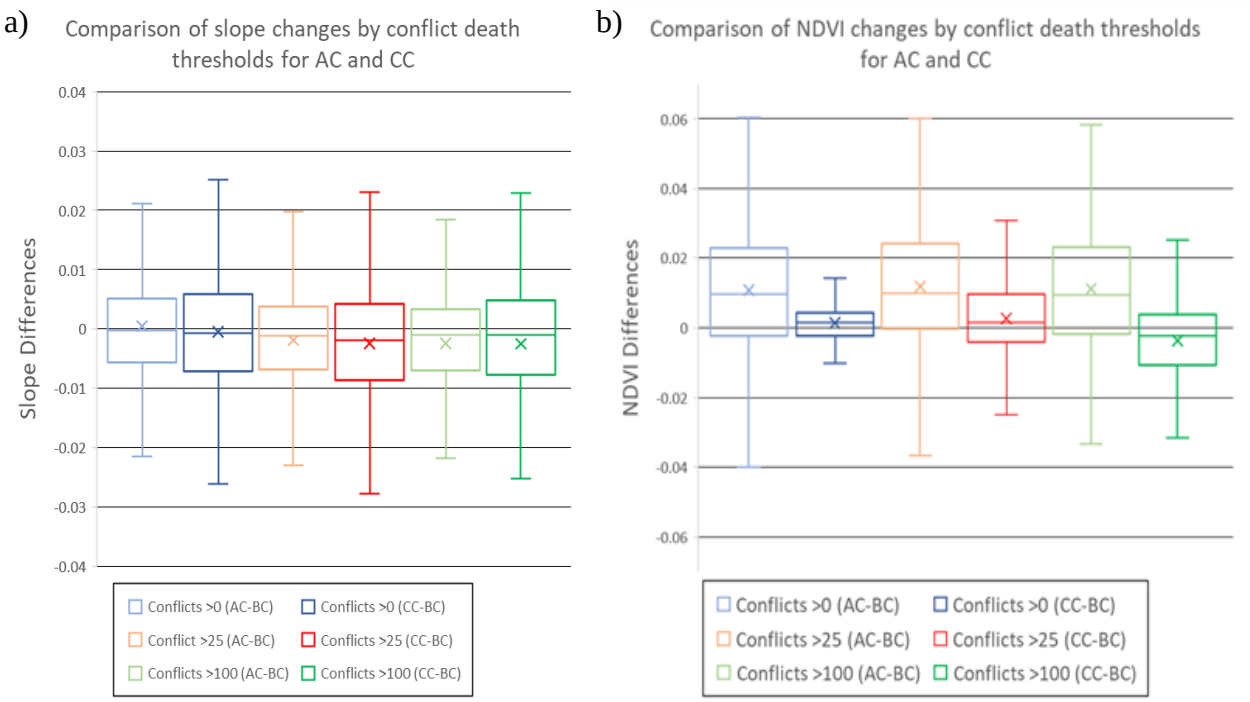

Figure 16 Comparison of a) slope changes and b) NDVI changes, for three conflict thresholds. The datasets include all global conflicts >25 deaths for the study period. For each threshold, both, observed (dull colors = AC-BC) and climate controlled (rich colors = CC-BC) are shown.

all six datasets show slight negative tendencies, while having almost the entire upper half of each dataset (inner box) in the positive region.

Large differences however can be seen between the observed NDVI changes (AC-BC) and the predicted NDVI changes (CC-BC) with much larger range (IQR, and extrema) of values. The different conflict death thresholds (>0, >25, >100) for the observed NDVI (AC-BC) datasets, show only small disparities (Fig 16b). Note, that all three datasets consist of comparably many conflicts. Similar to the other results, the CC-BC NDVI differences are mostly smaller than the observed differences and there is generally less variation.

6 Discussion

6.1 Impact of conflicts on vegetation greenness on global scale

The findings of the global (deaths >25) analysis, indicate, on average, an overall negative impact of conflicts on vegetation. However, the other statistical indicators document a strong variation in both NDVI and slope changes, which does not allow to conclude, with significance, on an overall influence in any direction. This is somewhat expected due to the heterogeneity of the conflicts involved in this study, considering the global and long-term scale of the dataset. Global vegetation studies using NDVI found either an overall increase in greening (Wang et al. 2018) due to climate change, changing land-management and other factors or overall negative trends (Fensholt and Proud 2012). Studies on regions found differing results; Forkel et al. (2013) for instance found that greening trends are positive in high latitudes, with increasing temperature in these parts and an expansion of shrubs in the arctic tundra. With the results not showing significant negative trends the hypothesis of overall negative impacts of conflicts on vegetation cannot be supported.

Still the overall results give diffuse signals for global conflict regions, which is not surprising comparing them to the other global studies (Wang et al. 2018; Fensholt and Proud 2012). However, since these studies (Wang et al. 2018; Fensholt and Proud 2012) look at global vegetation patterns, whereas this study uses rather several agglomerations of conflicts for some regions, it makes sense to look closer on these regions to answer why no significant increases or decreases is found. In a global dataset, regional patterns in vegetation greening are averaged out, by the usage of means. Vegetation growth depends strongly on regional conditions and doesn't change homogeneously over time and space. Zhang et al. (2013) for instance found that growing

season NDVI trends changed several times over a 1982-2011 year period, using a break-point analysis.

Most of the conflicts are located in tropical regions in eastern Africa and in the arid Middle East (Fig 1), and since these two regions contributed relatively strong to the results, a closer look on these parts of the world might lead to a better understanding of the results. Zaitchik et al. (2007) finds that vegetation in the Euphrates Plain (Middle East) is limited mainly by soil moisture. Climate variability therefore has strong impacts on this water-stressed region. Due to a prognosed decrease in precipitation and increase in temperature for the Middle East (IPCC 2008), the SM will become an even stronger limiting factor (Faour et al. 2016). Another study finds that the observed decrease in vegetation cover in the Middle East of -5% to -15% is mainly caused by human activities such as urban expansion (Faour et al. 2016). Conflicts can indirectly affect NDVI in dry regions, where agriculture depends on irrigation, by causing interruptions, leading to yield loss, as a study by Jaafar et al. (2015) focusing on the Syrian conflict found. Moreover, Forkel et al. (2013) finds that negative greening, or so called 'browning' is in some regions caused by water vapor pressure (Kawabata et al. 2001). For East Africa a GIMMS-based break point analysis revealed an overall negative NDVI trend from 1982 to 1998 and a positive trend from 1998 to 2015 (Kalisa et al. 2019). Additionally, it is concluded in the study, that NDVI for this region has a nonlinear response to climate.

Note that positive NDVI trends do not naturally imply a healthier environment. The reason for NDVI trend changes can lie in indirect or non-conflict related dynamics such as demographic or economic changes, leading to land-use changes, intensified agricultural production or simply de- or reforestation (Wang et al. 2018). Even though these effects were observed in the past, other factors could play key roles for both the negative and positive trend results. A potential conflict related explanation for positive trends could be the 'release effect' by conflict induced migration, resulting in decreased human pressure on ecosystems by reduced water or wood exploitation (Hanson et al. 2009).

It must be noted that vegetation health is not only a function of its ability to absorb light, which is the base of every VI. Other indicators such as biodiversity and the ability of plants to defend themselves against herbivores or other stress factors, also give important insights on the status. Additionally, interaction between flora and fauna, which depend and benefit from their mutual existence, play a key role for ecosystems and their resilience against shocks (Valiente-Banuet et

al. 2015). Since many conflicts take place in biodiversity hotspots, the effects of these factors are important to assess, especially in times of decreasing global biodiversity. These kinds of negative effects on ecosystems cannot be detected by spectral signals but could have long-term effects on vegetation.

6.1.1 Impact of climate change on vegetation greenness

Surface temperature, precipitation and soil moisture are key factors dominating vegetation growth and are used in this study to evaluate the NDVI trends (Zaitchik et al. 2007; Kawabata et al. 2001). As figure 11 displays, strong correlations between the mean changes of annual maximum temperature and annual maximum soil moisture are found. Nevertheless, precipitation which other studies found to be strongly correlated with NDVI (Jaafar et al. 2015), did not show a correlation with NDVI on this scale. Therefore, it seems likely that precipitation does not reflect the actual effect of this variable. Other influence factors such as surface radiation, nutrient availability or the occurrence of extreme events might additionally explain the vegetation change (Potter and Brooks 1998; Fensholt and Proud 2012). Other studies also focused on spring phenology and photosynthetic primary production to measure vegetation greening (Wang et al. 2018). Moreover, climate limits vegetation differently depending on regional conditions as discussed above for East Africa and the Middle East. Additionally, vegetation types respond differently to climate variations. Broadleaf forests were found to uniformly increase in NDVI, grasslands and shrublands showed balanced greening and browning trends, and in tundras, increased greening is measured (Eastman et al. 2013). The usage of three global climate variables for various climate and topographical zones is therefore a simplification (Kawabata et al. 2001). There are various other climate datasets globally or for particular regions for temperature precipitation or other modelled and observed variables (Beck et al. 2017; Mueller et al. 2011; Wang and Zeng 2015).

As visible in table 3 there is a large discrepancy between the climate predicted NDVI median and mean and the observed AC NDVI median and mean. Contrary to the positive correlation between NDVI and T and NDVI and SM (Fig 11), the climate control model predicted lower NDVI CC values. This is likely caused by gaps in the climate data, combined with the method of the prediction model. When missing data is present in any of the climate variables or NDVI over the whole period, the correspondent conflict is excluded. This is done due to errors in the code, occurring if the length of the slope years didn't match the length of the other data, due to missing values. This procedure led to exclusion of many conflicts, which might have caused this difference.

An additional contributing factor could be the usage of precipitation in the prediction model, although it did not show a strong relationship with NDVI. The usage of annual maximum data for the NDVI is chosen as representation of the maximum amount of green vegetation for each grid cell. Therefore, maxima of the climate variables are calculated to include interannual variability over the slope periods. Nevertheless, intra-annual means of T, P and SM instead of maxima could have been used in comparison.

Limitations

Some weaknesses and uncertainties were identified while conducting this study. The most important will be discussed briefly in the following sections.

GIMMS and NDVI

NDVI, even though it is the most used vegetation index, bears weaknesses, such as its sensitivity to dark soil substrate or other background materials, which can lead to higher NDVI values (Liang and Wang 2020a), or its saturation in areas of high-density forests, mostly in tropical rainforests, which makes it indifferentiable across higher densities. In this study large areas had to be excluded due to this effect (see chapter 4.2.1.1). Nevertheless, due to its good quality and long-term and global availability NDVI is found to be the best option (Tian et al. 2015).

Additionally, the GIMMS dataset inherits noise and other weaknesses which are approached and improved in newer versions, like the here used NDVI3g (Pinzon and Tucker 2014). Evaluations by comparing it to other middle to coarse resolution global datasets such as MODIS, which started in 2000, and therefore has an overlapping time of 11 years, identified an overall agreement between the two datasets (Fensholt and Proud 2012).

Since the method only involves broad scale spectral information, large pixel sizes ($1/12^{th}$ degree), and the main tool is a widely discussed VI (Bannari et al. 1995; Chandra 2011; Ji and Peters 2007; Fensholt and Proud 2012), conclusions on the actual status of vegetation can only be drawn limitedly. Various VIs with strengths and weaknesses for different vegetation types, and temporal and spatial scales have been developed over time and might lead to differing results (Bannari et al. 1995).

Spatial and temporal scope

There is a temporal delay between a conflict and its ‘visible manifestation’. It can take hours to days to see short term environmental effects and months to years for long-term direct or indirect effects such as landcover and land-use changes (Witmer 2015). There is no differentiation for these

effects, due to the large scale of this study. Consequently, observed changes in NDVI cannot be attributed to conflicts with certainty. The actual manifestation of spectrally and remotely observable conflict induced greening changes must be tested on a small scale. Short-term changes are likely to be connected to direct environmental effects and more steady increasing distant changes are more likely to be connected to land-use change (Witmer 2015). Moreover, the determination of a minimum regression period of six years and a range in periods of six to seventeen years bears the chance of errors due to the inconsistency. Additionally, the conflict dates are representing the point in time for each event. However, conflicts can go on for months, years or even decades. Therefore, impacts of the war or armed conflict on the conflict area is likely not limited to the single event for which the slope is calculated, but rather is effected already before or after the particular event occurs.

As discussed above, the decision for using the GIMMS dataset is mainly based on its temporal and spatial extent. But the spatial resolution must be discussed. The base of this study is the assumption that conflicts, as points inside a 64 km^2 pixel, have spectrally visible impacts on the surrounding plants. These impacts however vary strongly and might only be measurable on certain scales, but no clear assessment can be given for this scale.

6.2 Effects of different types of conflict on vegetation greenness

No significant differences between conflict types could be seen in the results (Fig 13). This might be caused by the size of the datasets and the global scale, averaging minor effects out. This makes conclusions on impacts by types difficult. Therefore, further analysis focusing on single conflict types dominant in specific armed conflicts or wars and regional context might lead to clearer results.

The approach of analyzing vegetation change based on conflict types is novel and therefore no comparisons to existing literature can be made. Nevertheless, related literature focusing on regions and one of the types show that neither positive nor negative impacts of conflicts are found. A study by Durán et al. (2011) found that forest-related conflicts, like guerilla wars can lead to conservation or deforestation. A master thesis by Andersson (2006) on the Angolan civil war occurring with interludes, between 1975 and 2002 showed that land cover was overall negatively affected by the war (NDVI based change in vegetation vigor). But complex dynamics are emphasized, and positive trends are found as well in some locations with vegetation regenerating

likely due to land abandonment. Therefore, again, mixed signals are present at larger scales, but more specific trend changes can be seen at local scales.

6.3 Comparison of the Rwanda genocide and the Afghanistan War

Analyzing the Afghanistan (mixed trend tendency) and Rwanda (negative trend tendency) datasets, differences on regional scales can be seen. Note that the slope periods are divided by the conflict years, which in the Rwanda case is a specific year (1994) for the whole datasets, in opposition to varying conflict years for the other sections. This likely affected the slope estimates, since NDVI of the same years are compared and led to a small range of the slopes represented by a small IQR (Fig 14).

In opposite to a study by Ndayisaba et al. (2016) who calculated long-term NDVI trends for the whole landmass of Rwanda, based on MODIS and GIMMS NDVI and found mostly greening trends, insignificant (slight negative tending) trends were found in conflict areas. It is discussed that the precipitation station data for Rwanda is uncomplete due to the destruction of meteorological infrastructure during the genocide, which likely affects the TerraClimate precipitation estimation (Ndayisaba et al. 2016). The impact of the genocide on vegetation is mainly indirect, due to abandonment of farmland and large numbers of refugees (Rwaka 2014). For the period after 1994 a negative NDVI trend was found in a study focusing on the Rusizi district in southwestern Rwanda during the genocide (Rwaka 2014). Additionally, deforestation and biodiversity loss was connected to the genocide (Moodley et al. 2010).

In Afghanistan most of the data is filtered out by the threshold (>25 deaths). Meaning that most events involved small death numbers of about ~7.4 deaths per event in comparison to ~2016 deaths per event for Rwanda. Note that some Rwanda events were extremely deadly, pulling the ratio up significantly. For Afghanistan studies on central Eurasia and Afghanistan reveal an overall increasing but seasonally varying NDVI for the period 1982–1994, but no further increase since. The region is controlled mainly by precipitation and temperature (Xu et al. 2017). Hot spells and droughts are affecting the vegetation. A study on the effects of wars and droughts on NDVI in Afghanistan found that between 1995 and 2001 the decreasing NDVI was mainly caused by droughts, whereas a mixed trend signal was found for 2001 to 2005. The Soviet-Afghanistan War caused abandonment of agriculture due to mining, cutting of trees and migration led to long-term de-vegetation effects (de Beurs and Henebry 2008). The mixed signals for conflict regions are

therefore to other findings. However, the trend signals are difficult to assign to conflicts, since droughts appeared during the study period (2001 and 2008) (Rousta et al. 2020).

6.4 Effect of fatality number, extend of event

Concerning the severity of events, represented by conflict death numbers, neither significant trends nor significant differences between conflict slopes for the three death thresholds can be identified in the results. Looking at the mean NDVI changes, the same pattern as for the other results can be seen, with overall higher observed NDVI than predicted NDVI in the AC periods. It is somewhat surprising that larger scale conflicts seem not to visibly and measurably affect the surrounding environment. It is therefore assumed that the size and distribution of the datasets dominated the findings, similar to the other results. The larger the datasets, the likelier that positive and negative visible manifestations of conflicts offset each other. Furthermore, it is surprising that the majority of NDVI slopes in both directions and for all three thresholds, are noticeably low, ranging (IQR) between 0.01 and -0.01. Except for some outliers, which are excluded for visibility, all slopes change (AC-BC) are unexpectedly close to 0. Meaning that in the correspondent conflict regions almost no NDVI change is present over the study period.

Due to the specificity of the analysis, no direct comparison to other studies focusing on death thresholds can be performed.

7 Conclusions

No significant impact of conflicts could be found in any dataset. Eight out of nine overall slope difference means, and seven out of nine respective medians are negative (but insignificantly). The regional example of Rwanda shows a negative trend tendency, with ~75% of the slopes being negative. The method used is looking for statistical relationships and must account for the large temporal and spatial scope of this study. Cross validation of the identified trend indications with other VIs and data from other sensors to estimated vegetation and climate are needed, to further evaluate the results. More precision would likely be reached by selecting a region, where effects, type and duration of events are known with higher certainty. In that case the NDVI trend analysis could focus on the period of the war, and the long-term and short-term impacts could be differentiated.

In other research areas such as atmospheric science, anthropogenic impacts on the environment is evident, and is represented by the term ‘anthropogenic forcing‘ (Myhre et al. 2013) which includes land modification, as well as atmospheric changes due to fossil fuel-based greenhouse gas emissions. The results found in this analysis do not prove a negative impact of conflict-based anthropogenic forcing, but due to the discussed weaknesses of the method and data, to falsify the hypothesis, more research is needed.

Conflicts can have both positive and negative impacts, and this study did not find any significant global trend patterns, it is assumed that the impacts offset each other. It is therefore strongly recommended to focus on more regional scales in future studies, to assess under which circumstances the conflicts have positive and under which circumstances they have negative impact on the vegetation greening.

Lastly, the following statement motivated me and maybe motivates others to address this topic.

“*The changing nature of violent conflict, combined with long-term demographic, economic and environmental trends present significant practical challenges for global peace and security*” (UN-HABITAT 2012, p. 13).

8 References

Abatzoglou, J., S. Dobrowski, S. Parks, and K. Hegewisch. 2017. TerraClimate. Monthly Climate and Climatic Water Balance for Global Terrestrial Surfaces. Retrieved 15.09. 2020, from. https://developers.google.com/earth-engine/datasets/catalog/IDAHO_EPSCOR_TERRACLIMATE#bands

Abatzoglou, J. T., S. Z. Dobrowski, S. A. Parks, and K. C. Hegewisch. 2018. TerraClimate, a high-resolution global dataset of monthly climate and climatic water balance from 1958–2015. *Scientific data,* 5**:** 170191.

Al Ajmi, D. 2009. Remote sensing: fundamentals, types and monitoring applications of environmental consequences of war. In *Environmental Consequences of War and Aftermath*, 41-124 pp.: Springer.

Andersson, J. 2006. Land cover change in the Okavango River Basin: Historical changes during the Angolan civil war, contributing causes and effects on water quality. Tema vatten i natur och samhälle.

Anson, P., and D. Cummings. 1991. The first space war: the contribution of satellites to the Gulf War. *The RUSI Journal,* 136**:** 45-53.

Bannari, A., D. Morin, F. Bonn, and A. Huete. 1995. A review of vegetation indices. *Remote sensing reviews,* 13**:** 95-120.

Baumann, M., and T. Kuemmerle. 2016. The impacts of warfare and armed conflict on land systems. *Journal of Land Use Science,* 11**:** 672-688. DOI: 10.1080/1747423x.2016.1241317

Beck, H. E., N. Vergopolan, M. Pan, V. Levizzani, A. I. Van Dijk, G. P. Weedon, L. Brocca, F. Pappenberger, et al. 2017. Global-scale evaluation of 22 precipitation datasets using gauge observations and hydrological modeling. *Hydrology and Earth System Sciences,* 21**:** 6201-6217.

Beck, P. S., C. Atzberger, K. A. Høgda, B. Johansen, and A. K. Skidmore. 2006. Improved monitoring of vegetation dynamics at very high latitudes: A new method using MODIS NDVI. *Remote sensing of Environment,* 100**:** 321-334.

Beck, P. S., and S. J. Goetz. 2011. Satellite observations of high northern latitude vegetation productivity changes between 1982 and 2008: ecological variability and regional differences. *Environmental Research Letters,* 6**:** 045501.

Box, E. O., B. N. Holben, and V. Kalb. 1989. Accuracy of the AVHRR vegetation index as a predictor of biomass, primary productivity and net CO 2 flux. *Vegetatio,* 80**:** 71-89.

Bromley, L. 2010. Relating violence to MODIS fire detections in Darfur, Sudan. *International Journal of Remote Sensing,* 31**:** 2277-2292.

Brown, I. A. 2010. Assessing eco-scarcity as a cause of the outbreak of conflict in Darfur: a remote sensing approach. *International Journal of Remote Sensing,* 31**:** 2513-2520. DOI: 10.1080/01431161003674592

Brundtland, G. H. 1987. Our common future, report of the World Commission on Environment and Development, World commission on environment and development, 1987. *Published as Annex to General Assembly document A/42/427, development and international Co-operation: Environment August,* 2**:** 1987.

Byers, M., and N. Dragojlovic. 2004. Darfur: a climate change-induced humanitarian crisis? *Human Security Bulletin***:** 16-18.

Chan, K. M., M. R. Shaw, D. R. Cameron, E. C. Underwood, and G. C. Daily. 2006. Conservation planning for ecosystem services. *PLoS biology,* 4.

Chandra, P. 2011. Performance evaluation of vegetation indices using remotely sensed data. *International Journal of Geomatics and Geosciences,* 2**:** 231-240.

de Beurs, K., G. Ioffe, T. Nefedova, and G. Henebry. 2017. Land Change in European Russia: 1982–2011. In *Land-Cover and Land-Use Changes in Eastern Europe after the Collapse of the Soviet Union in 1991*, 223-241 pp.: Springer.

de Beurs, K. M., and G. M. Henebry. 2008. War, drought, and phenology: changes in the land surface phenology of Afghanistan since 1982. *Journal of Land Use Science,* 3**:** 95-111.

Ding, M., Y. Zhang, L. Liu, W. Zhang, Z. Wang, and W. Bai. 2007. The relationship between NDVI and precipitation on the Tibetan Plateau. *Journal of Geographical Sciences,* 17**:** 259-268.

Dinh, H. 1984. Long-term changes in dense inland forest following herbicidal attack. 1984. *Herbicides in war: the long-term ecological and human consequences. Stockholm International Peace Research Institute. Taylor & Francis, London***:** 31-32.

Dudley, J. P., J. R. Ginsberg, A. J. Plumptre, J. A. Hart, and L. C. Campos. 2002. Effects of War and Civil Strife on Wildlife and Wildlife Habitats. *Conservation Biology,* 16.

Durán, E., D. B. Bray, A. Velázquez, and A. Larrazábal. 2011. Multi-scale forest governance, deforestation, and violence in two regions of Guerrero, Mexico. *World Development,* 39**:** 611-619.

Escobar, H. 2019. Brazilian president attacks deforestation data. American Association for the Advancement of Science.

Faour, G., M. Mhawej, and A. Fayad. 2016. Detecting Changes in Vegetation Trends in the Middle East and North Africa (MENA) Region Using SPOT Vegetation. *Cybergeo: European Journal of Geography*.

Fensholt, R., and S. R. Proud. 2012. Evaluation of earth observation based global long term vegetation trends—Comparing GIMMS and MODIS global NDVI time series. *Remote sensing of Environment,* 119**:** 131-147.

Fernandes, P. M., and H. S. Botelho. 2003. A review of prescribed burning effectiveness in fire hazard reduction. *International Journal of wildland fire,* 12**:** 117-128.

Fisher, B., and R. K. Turner. 2008. Ecosystem services: classification for valuation. *Biological conservation,* 141**:** 1167-1169.

Flint, J. 2009. *Beyond" Janjaweed": Understanding the Militias of Darfur*. Small Arms Survey.

Forkel, M., N. Carvalhais, J. Verbesselt, M. Mahecha, C. Neigh, and M. Reichstein. 2013. Trend Change Detection in NDVI Time Series: Effects of Inter-Annual Variability and Methodology. *Remote Sensing,* 5**:** 2113-2144. DOI: 10.3390/rs5052113

Francis, R. A., and K. Krishnamyrthy. 2014. Human conflict and ecosystem services. Finding the environmental price of warfare. *International Affairs,* 90**:** 853–869.

Gebhardt, H., R. Glaser, U. Radtke, P. Reuber, and A. Vött. 2007. Niederschlagsbildung und Niederschlagsvariabilität. In *Geographie: Physische Geographie und Humangeographie*, 573-575 pp. Heidelberg: Spektrum.

Gleditsch, N. P. 1998. Armed conflict and the environment: A critique of the literature. *Journal of peace research,* 35**:** 381-400.

Gleditsch, N. P., P. Wallensteen, M. Eriksson, M. Sollenberg, and H. Strand. 2002. Armed conflict 1946-2001: A new dataset. *Journal of peace research,* 39**:** 615-637.

Gorsevski, V., E. Kasischke, J. Dempewolf, T. Loboda, and F. Grossmann. 2012. Analysis of the Impacts of armed conflict on the Eastern Afromontane forest region on the South Sudan—Uganda border using multitemporal Landsat imagery. *Remote Sensing of Environment,* 118**:** 10-20.

Guo, X., H. Zhang, Z. Wu, J. Zhao, and Z. Zhang. 2017. Comparison and evaluation of annual NDVI time series in China derived from the NOAA AVHRR LTDR and Terra MODIS MOD13C1 products. *Sensors,* 17**:** 1298.

Gutman, G. G. 1999. On the use of long-term global data of land reflectances and vegetation indices derived from the advanced very high resolution radiometer. *Journal of Geophysical Research: Atmospheres,* 104**:** 6241-6255. DOI: 10.1029/1998jd200106

Hanson, T., T. M. Brooks, G. A. B. Da Fonseca, M. Hoffmann, J. F. Lamoreux, G. Machlis, C. G. Mittermeier, R. A. Mittermeier, et al. 2009. Warfare in biodiversity hotspots. *Conserv Biol,* 23**:** 578-587. DOI: 10.1111/j.1523-1739.2009.01166.x

Harris, I., P. D. Jones, T. J. Osborn, and D. H. Lister. 2014. Updated high-resolution grids of monthly climatic observations–the CRU TS3. 10 Dataset. *International journal of climatology,* 34**:** 623-642.

Hijmans, R. J., S. E. Cameron, J. L. Parra, P. G. Jones, and A. Jarvis. 2005. Very high resolution interpolated climate surfaces for global land areas. *International Journal of Climatology: A Journal of the Royal Meteorological Society,* 25**:** 1965-1978.

Högbladh, S. 2020. UCDP Georeferenced Event Dataset Codebook Version 20.1. Uppsala Conflict Data Program. Department of Peace and Conflict Research: Uppsala University.

Holben, B. N. 1986. Characteristics of maximum-value composite images from temporal AVHRR data. *International Journal of Remote Sensing,* 7**:** 1417-1434. DOI: 10.1080/01431168608948945

Huete, A. 1988. A Soil-Adjusted Vegetation Index (SAVI). Remote Ssensing of Environment, 25, 295-309.

Ichii, K., A. Kawabata, and Y. Yamaguchi. 2002. Global correlation analysis for NDVI and climatic variables and NDVI trends: 1982-1990. *International journal of remote sensing,* 23**:** 3873-3878.

IPCC, 2008. Technical paper. Accessed on 15th October 2020. Report. [in Swedish, English summary]

IPCC. 2013. Hartmann, D.L., A.M.G. Klein Tank, M. Rusticucci, L.V. Alexander, S. Brönnimann, Y. Charabi, F.J. Dentener, E.J. Dlugokencky, D.R. Easterling, A. Kaplan, B.J. Soden, P.W. Thorne, M. Wild and P.M. Zhai, Observations: Atmosphere and Surface. In: Climate Change 2013: The Physical Science Basis. Contribution of Working Group I to the Fifth Assessment Report of the Intergovernmental Panel on Climate Change. [Stocker, T.F., D. Qin, G.-K. Plattner, M. Tignor, S.K. Allen, J. Boschung, A. Nauels, Y. Xia, V. Bex and P.M. Midgley (eds.)]. Cambridge University
Press, Cambridge, United Kingdom and New York, NY, USA.
.

IPCC. 2019. Climate Change and Land: an IPCC special report on climate change, desertification, land degradation, sustainable land management, food security, and greenhouse gas fluxes in terrestrial ecosystems. *P.R. Shukla, J. Skea, E. Calvo Buendia, V. Masson-Delmotte, H.-O. Pörtner, D. C. Roberts, P.*

Zhai, R. Slade, S. Connors, R. van Diemen, M. Ferrat, E. Haughey, S. Luz, S. Neogi, M. Pathak, J. Petzold, J. Portugal Pereira, P. Vyas, E. Huntley, K. Kissick, M. Belkacemi, J. Malley, (eds.)]. In press.

Jaafar, H. H., R. Zurayk, C. King, F. Ahmad, and R. Al-Outa. 2015. Impact of the Syrian conflict on irrigated agriculture in the Orontes Basin. *International Journal of Water Resources Development,* 31**:** 436-449.

Ji, L., and A. J. Peters. 2004. A spatial regression procedure for evaluating the relationship between AVHRR-NDVI and climate in the northern Great Plains. *International Journal of Remote Sensing,* 25**:** 297-311.

Ji, L., and A. J. Peters. 2007. Performance evaluation of spectral vegetation indices using a statistical sensitivity function. *Remote Sensing of Environment,* 106**:** 59-65.

Jönsson, P., and L. Eklundh. 2004. TIMESAT—a program for analyzing time-series of satellite sensor data. *Computers & geosciences,* 30**:** 833-845.

Kalisa, W., T. Igbawua, M. Henchiri, S. Ali, S. Zhang, Y. Bai, and J. Zhang. 2019. Assessment of climate impact on vegetation dynamics over East Africa from 1982 to 2015. *Scientific reports,* 9**:** 1-20.

Kawabata, A., K. Ichii, and Y. Yamaguchi. 2001. Global monitoring of interannual changes in vegetation activities using NDVI and its relationships to temperature and precipitation. *International journal of remote sensing,* 22**:** 1377-1382.

Kern, A., H. Marjanović, and Z. Barcza. 2016. Evaluation of the Quality of NDVI3g Dataset against Collection 6 MODIS NDVI in Central Europe between 2000 and 2013. *Remote Sensing,* 8**:** 955.

Kim, K. C. 1997. Preserving Biodiversity in Korea's Demilitarized Zone. *Science,* 278.

Kobayashi, S., Y. Ota, Y. Harada, A. Ebita, M. Moriya, H. Onoda, K. Onogi, H. Kamahori, et al. 2015. The JRA-55 reanalysis: General specifications and basic characteristics. *Journal of the Meteorological Society of Japan. Ser. II,* 93**:** 5-48.

Le Treut, H., and R. Somerville. 2007. Chapter 1: Historical overview of climate change science. *IPCC Fourth Assessment Review: Climate Change Science*.

Levy, R. 2000. NASA. Earth Observatory. Measuring Vegetation (NDVI & EVI). Enhanced Vegetation Index (EVI) Retrieved 06.09 2020, from. https://earthobservatory.nasa.gov/features/MeasuringVegetation/measuring_vegetation_4.php

Liang, S., and J. Wang. 2020a. Chapter 10 - Leaf area index. In *Advanced Remote Sensing (Second Edition),* eds. S. Liang, and J. Wang, 405-445 pp.: Academic Press.

Liang, S., and J. Wang. 2020b. Chapter 14 - Aboveground biomass. In *Advanced Remote Sensing (Second Edition),* eds. S. Liang, and J. Wang, 543-580 pp.: Academic Press.

Liu, H., P. Gong, J. Wang, N. Clinton, Y. Bai, and S. Liang. 2019. Annual Dynamics of Global Land Cover and its Long-term Changes from 1982 to 2015. DOI: 10.5194/essd-2019-23

Liu, Y., Y. Li, S. Li, and S. Motesharrei. 2015. Spatial and temporal patterns of global NDVI trends: correlations with climate and human factors. *Remote Sensing,* 7**:** 13233-13250.

Martin, P. S., and C. R. Szuter. 1999. War zones and game sinks in Lewis and Clark's west. *Conservation Biology,* 13**:** 36-45.

Maystadt, J.-F., V. Mueller, J. Van Den Hoek, and S. van Weezel. 2020. Vegetation changes attributable to refugees in Africa coincide with agricultural deforestation. *Environmental Research Letters*. DOI: 10.1088/1748-9326/ab6d7c

McNeely, J. A. 2003. Conserving forest biodiversity in times of violent conflict. *Oryx,* 37**:** 142-152.

Moodley, V., A. Gahima, and S. Munien. 2010. Environmental causes and impacts of the genocide in Rwanda: Case studies of the towns of Butare and Cyangugu. *African Journal on Conflict Resolution,* 10.

Mueller, B., S. I. Seneviratne, C. Jimenez, T. Corti, M. Hirschi, G. Balsamo, P. Ciais, P. Dirmeyer, et al. 2011. Evaluation of global observations-based evapotranspiration datasets and IPCC AR4 simulations. *Geophysical Research Letters,* 38.

Müller, D., Z. Sun, T. Vongvisouk, D. Pflugmacher, J. Xu, and O. Mertz. 2014. Regime shifts limit the predictability of land-system change. *Global Environmental Change,* 28**:** 75-83.

Myhre, G., D. Shindell, F.-M. Bréon, W. Collins, J. Fuglestvedt, J. Huang, D. Koch, J.-F. Lamarque, et al. 2013. Anthropogenic and Natural Radiative Forcing. In: Climate Change 2013: The Physical Science Basis. Contribution of Working Group I to the Fifth Assessment Report of the Intergovernmental Panel on Climate Change [Stocker, T.F., D. Qin, G.-K. Plattner, M. Tignor, S.K. Allen, J. Boschung, A. Nauels, Y. Xia, V. Bex and P.M. Midgley (eds.)]. Cambridge University Press, Cambridge, United Kingdom and New York, NY, USA.

Ndayisaba, F., H. Guo, A. Bao, H. Guo, F. Karamage, and A. Kayiranga. 2016. Understanding the spatial temporal vegetation dynamics in Rwanda. *Remote Sensing,* 8**:** 129.

Nietschmann, B. 1990. Battlefields of ashes and mud. *Natural History,* 99**:** 35-37.

NOAA. 2020a. Climate at a Glance: Global Time Series. National Oceanic and Amtomsphereic Administration. National Centers for Environmental information.

NOAA. 2020b. Climate Change Indicators: U.S. and Global Precipitation. National Oceanic and Amtomsphereic Administration. National Centers for Environmental information.

NOAA. 2020c. State of the Climate: Global Climate Report for 2019. National Oceanic and Amtomsphereic Administration. National Centers for Environmental information.

Oppenheimer, M., M. Campos, R. Warren, J. Birkmann, G. Luber, B. O'Neill, K. Takahashi, M. Brklacich, et al. 2015. Emergent risks and key vulnerabilities. In *Climate Change 2014 Impacts, Adaptation and Vulnerability: Part A: Global and Sectoral Aspects*, 1039-1100 pp.: Cambridge University Press.

Pei, Z., S. Fang, W. Yang, L. Wang, M. Wu, Q. Zhang, W. Han, and D. N. Khoi. 2019. The relationship between NDVI and climate factors at different monthly time scales: a case study of grasslands in inner Mongolia, China (1982–2015). *Sustainability,* 11**:** 7243.

Pettersson, T., and P. Wallensteen. 2015. Armed conflicts, 1946–2014. *Journal of peace research,* 52**:** 536-550.

Pinzon, J., and C. Tucker. 2014. A Non-Stationary 1981–2012 AVHRR NDVI3g Time Series. *Remote Sensing,* 6**:** 6929-6960. DOI: 10.3390/rs6086929

Potter, C., and V. Brooks. 1998. Global analysis of empirical relations between annual climate and seasonality of NDVI. *International Journal of Remote Sensing,* 19**:** 2921-2948.

Prescott, G. W., W. J. Sutherland, D. Aguirre, M. Baird, V. Bowman, J. Brunner, G. M. Connette, M. Cosier, et al. 2017. Political transition and emergent forest-conservation issues in Myanmar. *Conservation Biology,* 31**:** 1257-1270.

Rabinowitz, A. 2005. Guns, Gold, and Greed: Protecting tigers in the farthest reaches of Myanmar. *WILDLIFE CONSERVATION,* 108**:** 18.

Raleigh, C., and H. Urdal. 2007. Climate change, environmental degradation and armed conflict. *Political Geography,* 26**:** 674-694. DOI: 10.1016/j.polgeo.2007.06.005

Rockström, J., W. Steffen, K. Noone, Å. Persson, F. S. Chapin, E. F. Lambin, T. M. Lenton, M. Scheffer, et al. 2009. A safe operating space for humanity. *nature,* 461**:** 472-475.

Roser, M. 2016. War and Peace. OurWorldInData.org: Uppsala Conflict Data Program (UCDP).

Rousta, I., H. Olafsson, M. Moniruzzaman, H. Zhang, Y.-A. Liou, T. D. Mushore, and A. Gupta. 2020. Impacts of drought on vegetation assessed by vegetation indices and meteorological factors in Afghanistan. *Remote Sensing,* 12**:** 2433.

Rwaka, M. 2014. An attempt to investigate the impact of 1994 Tutsi Genocide in Rwanda on Landscape using Remote Sensing and GIS analysis. *Student thesis series INES*.

Schierhorn, F., D. Müller, T. Beringer, A. V. Prishchepov, T. Kuemmerle, and A. Balmann. 2013. Post-Soviet cropland abandonment and carbon sequestration in European Russia, Ukraine, and Belarus. *Global Biogeochemical Cycles,* 27**:** 1175-1185.

Schultz, P., and M. Halpert. 1993. Global correlation of temperature, NDVI and precipitation. *Advances in Space Research,* 13**:** 277-280.

Sellers, P. J. 1985. Canopy reflectance, photosynthesis and transpiration. *International journal of remote sensing,* 6**:** 1335-1372.

Shimabukuro, Y., V. Carvalho, and B. Rudorff. 1997. NOAA-AVHRR data processing for the mapping of vegetation cover. *International Journal of Remote Sensing,* 18**:** 671-677.

Smith, J. W., G. Lyons, and G. Sauer-Thompson. 1999. Civilization's wake: Ecology, economics and the roots of environmental destruction and neglect. In *The Bankruptcy of Economics: Ecology, Economics and the Sustainability of the Earth*, 89-126 pp.: Springer.

Smith, T. D. 1996. Scaling Fisheries: The Science of Measuring the Effects of Fishing, 1855-1955.

Stevens, K., L. Campbell, G. Urquhart, D. Kramer, and J. Qi. 2011. Examining complexities of forest cover change during armed conflict on Nicaragua's Atlantic Coast. *Biodiversity and Conservation,* 20**:** 2597-2613.

Sundberg, R., and E. Melander. 2013a. Introducing the UCDP georeferenced event dataset. *Journal of Peace Research,* 50**:** 523-532.

Sundberg, R., and E. Melander. 2013b. UCDP Georeferenced Event Dataset (GED) Global. ed. UCDP. Journal of Peace Research: Department of Peace and Conflict Research.

Tagesson, T., R. Fensholt, B. Cappelaere, E. Mougin, S. Horion, L. Kergoat, H. Nieto, C. Mbow, et al. 2016. Spatiotemporal variability in carbon exchange fluxes across the Sahel. *Agricultural and Forest Meteorology,* 226**:** 108-118.

Taub, D. 2010. Effects of Rising Atmospheric Concentrations of Carbon Dioxide on Plants. *Nature Education Knowledge,* 3.

Tian, F., R. Fensholt, J. Verbesselt, K. Grogan, S. Horion, and Y. Wang. 2015. Evaluating temporal consistency of long-term global NDVI datasets for trend analysis. *Remote Sensing of Environment,* 163**:** 326-340.

Tucker, C. J. 1979. Red and photographic infrared linear combinations for monitoring vegetation. *Remote sensing of Environment,* 8**:** 127-150.

Tucker, C. J., J. E. Pinzon, M. E. Brown, D. A. Slayback, E. W. Pak, R. Mahoney, E. F. Vermote, and N. El Saleous. 2005. An extended AVHRR 8-km NDVI dataset compatible with MODIS and SPOT vegetation NDVI data. *International Journal of Remote Sensing,* 26**:** 4485-4498.

UCDP. 2019. Bulletin. "Afghanistan: The deadliest conflict in the world.".

UCDP. 2020a. Georeferenced Event Dataset (GED) Global version 19.1. Department of Peace and Conflict Research: Uppsala University.

UCDP. 2020b. Uppsala Conflict Data Program (UCDP). Retrieved 04.03 2020, from. https://www.pcr.uu.se/research/ucdp/

UN-HABITAT. 2012. Toolkit and Guidance for Preventing and Managing Land and Natural Resources Conflict: Land and Conflict. p. 13. New York: United Nations Interagency Framework Team for Preventive Action.

Urdal, H. 2005. People vs. Malthus: Population pressure, environmental degradation, and armed conflict revisited. *Journal of Peace Research,* 42**:** 417-434.

Valiente-Banuet, A., M. A. Aizen, J. M. Alcántara, J. Arroyo, A. Cocucci, M. Galetti, M. B. García, D. García, et al. 2015. Beyond species loss: the extinction of ecological interactions in a changing world. *Functional Ecology,* 29**:** 299-307.

Wang-Erlandsson, L., W. G. Bastiaanssen, H. Gao, J. Jagermeyr, G. B. Senay, A. Van Dijk, J. P. Guerschman, P. W. Keys, et al. 2016. Global root zone storage capacity from satellite-based evaporation.

Wang, A., and X. Zeng. 2015. Global hourly land surface air temperature datasets: inter-comparison and climate change. *International Journal of Climatology,* 35**:** 3959-3968.

Wang, L., F. Tian, Y. Wang, Z. Wu, G. Schurgers, and R. Fensholt. 2018. Acceleration of global vegetation greenup from combined effects of climate change and human land management. *Global Change Biology,* 24**:** 5484-5499. DOI: 10.1111/gcb.14369

Werth, D., and R. Avissar. 2002. The local and global effects of Amazon deforestation. *Journal of Geophysical Research: Atmospheres,* 107**:** LBA 55-51-LBA 55-58.

Witmer, F. D. W. 2015. Remote sensing of violent conflict: eyes from above. *International Journal of Remote Sensing,* 36**:** 2326-2352. DOI: 10.1080/01431161.2015.1035412

Witte, G. 2018. Afghanistan War. 2001–2014. *Encyclopedia Britannica, www. brittannica. com Accessed at: http://www. britannica. com/event/Afghanistan-War*.

Xu, H.-j., X.-p. Wang, and T.-b. Yang. 2017. Trend shifts in satellite-derived vegetation growth in Central Eurasia, 1982–2013. *Science of the Total Environment,* 579**:** 1658-1674.

Xue, J., and B. Su. 2017. Significant remote sensing vegetation indices: A review of developments and applications. *Journal of Sensors,* 2017.

Zaitchik, B. F., J. P. Evans, R. A. Geerken, and R. B. Smith. 2007. Climate and vegetation in the Middle East: Interannual variability and drought feedbacks. *Journal of Climate,* 20**:** 3924-3941.

Zeng, H., G. Jia, and H. Epstein. 2011. Recent changes in phenology over the northern high latitudes detected from multi-satellite data. *Environmental Research Letters,* 6**:** 045508.

Zhang, Y., J. Gao, L. Liu, Z. Wang, M. Ding, and X. Yang. 2013. NDVI-based vegetation changes and their responses to climate change from 1982 to 2011: A case study in the Koshi River Basin in the middle Himalayas. *Global and Planetary Change,* 108**:** 139-148.

Zhang, Y., X. Xiao, X. Wu, S. Zhou, G. Zhang, Y. Qin, and J. Dong. 2017. A global moderate resolution dataset of gross primary production of vegetation for 2000–2016. *Scientific data,* 4**:** 170165.

Zhu, X., and D. Liu. 2015. Improving forest aboveground biomass estimation using seasonal Landsat NDVI time-series. *ISPRS Journal of Photogrammetry and Remote Sensing,* 102**:** 222-231.